Received: 8 August 2023 | Revised: 18 December 2023 | Accepted: 22 December 2023

DOI: 10.1002/ese3.1673

ORIGINAL ARTICLE

Parameter identification of solar photovoltaic models by multi strategy sine–cosine algorithm

Ting-ting Zhou[1] | **Chao Shang**[2]

[1]Architectural Engineering Institute, Maanshan University, Maanshan, China

[2]Pujiang Institute, Nanjing Tech University, Nanjing, China

Correspondence
Ting-ting Zhou, Architectural Engineering Institute, Maanshan University, 243100 Maanshan, China.
Email: echo6020100@163.com

Abstract

Accurate modeling and parameter identification of photovoltaic (PV) cells is a difficult task due to the nonlinear characteristics of PV cells. The goal of this paper is to propose a multi strategy sine–cosine algorithm (SCA), named enhanced sine–cosine algorithm (ESCA), to evaluate nondirectly measurable parameters of PV cells. The ESCA introduces the concept of population average position to increase the population exploration ability, and at the same time introduces the personal destination agent mutation mechanism and competitive selection mechanism into SCA to provide more search directions for ESCA while ensuring the search accuracy and diversity maintenance. To prove that the proposed ESCA is the best choice for extracting nondirectly measurable parameters of PV cells, ESCA is evaluated by the single-diode model, the double-diode model, the three-diode model, and the photovoltaic module model (PVM), and compared with eight existing popular methods. Experimental results show that ESCA outperforms similar methods in terms of diversity maintenance, high efficiency, and stability. In particular, the proposed ESCA method is less than the SCA by 0.081, 0.144, and 0.578 in the standard deviation statistics metrics of the three PVM models (PVPWP201, STM6-40/36, and STP6-120/36), respectively. Therefore, the proposed ESCA is an accurate and reliable method for parameter identification of PV cells.

KEYWORDS

mutation mechanism, parameter identification, photovoltaic cells, sine–cosine algorithm

1 | INTRODUCTION

In recent years, with the rapid development of society and economy, the human's demand for energy has been increasing day by day.[1] Coal- and oil-based fossil energy will produce a large number of pollutants such as carbon dioxide, sulfur oxides, and nitrogen oxides during the use process, resulting in inestimable environmental losses and inevitably causing frequent occurrences of extreme climates. Therefore, it is extremely urgent to find a clean and pollution-free alternative energy source.[2] Many researchers have found many alternatives to traditional energy sources, mainly including three categories: hydropower, wind energy, and solar energy. Solar energy

has the advantages of being renewable, low in cost, and having little negative impact on the environment, and has been valued by many countries and has gradually broken the monopoly of traditional fossil energy.[3] At the same time, with the in-depth research on the performance of photovoltaic (PV) cell raw materials by many researchers, the price of solar cells has dropped sharply, which makes solar energy more and more recognized by most people.[4]

Estimation of PV cell model parameters is an important topic in PV systems.[5–7] Accurate identification of PV model parameters is essential for assessing the performance of solar PV systems. These parameters can help determine the actual operating state of the system, thus enabling performance optimization and enhancement. In actual operation, it is difficult to obtain real and sufficient data for parameter identification, especially under different environmental conditions such as light irradiance and temperature,[8,9] the variability of data collection is high, and the behavior of the PV system is affected by many factors such as temperature, light irradiance, which makes the PV model structure complex with multiple nonlinear parameters, and undoubtedly makes the PV model parameter identification difficult. In addition, important parameters such as current, resistance, and diode ideality factor inside PV cells are not available directly from the manufacturer. Recognized PV cell models mainly include the single-diode model (SDM), the double-diode model (DDM), and the three-diode model (TDM),[10] and the corresponding solution methods of the models are mainly divided into heuristic algorithms and deterministic algorithms. The deterministic algorithm mainly adopts the mathematical programming method in operations research, and the estimation result of the model parameters is overly dependent on the selection of the initial value.[11] The heuristic algorithm[12,13] is not limited by the traditional mathematical solution rules to solve the problem, which searches through random behavior and has achieved recognized results in the field of PV parameter identification. Zhou et al.[14] proposed an adaptive differential evolution algorithm based on a dynamic opposite learning strategy to effectively extract the optimal parameters of different PV cell models. Xu et al.[15] presented an improved political optimizer that enhances overall equilibrium and local exploitability by introducing quantum rotation gate and Nelder–Mead simplex (NMs) strategies into the parameter evaluation process. Bo et al.[16] introduced a robust niching chimp optimization, which uses niche technology and new constraint-handling methods to improve the searchability and robustness of the algorithm. Yang et al.[17] proposed a hybrid and efficient chimp algorithm and applied it effectively on three widely used commercial photovoltaic modules (PVMs). El-Dabah et al.[18] presented a Northern Goshawk Optimization, which accurate description of nonlinear current–voltage characteristic curve behavior by the TDM of a PVM.

Although the above solution techniques have achieved varying degrees of success, the difficulty in parameter setting of these methods and the lack of design considerations for some optimization problems make them show different degrees of optimization deficiency in finding the optimal solution.[19–22] Thankfully, a series of heuristic algorithms with advanced theories have been successively proposed, including monarch butterfly optimization,[23] moth search algorithm,[24] hunger games search (HGS),[25] Runge–Kutta method,[26] colony predation algorithm,[27] weighted mean of vectors,[28] Harris Hawks Optimization (HHO),[29] rime optimization algorithm (RIME),[30] and the sine–cosine algorithm (SCA).[31] In addition, a number of combinatorial algorithms have been recognized, such as BOAALO[32] based on butterfly optimization algorithm,[33] and ant lion optimizer[34]; CNNA-BES[35] based on convolutional neural network architecture and bald eagle search[36] optimization algorithm; QGBWOA[37] based on quasi-opposition-based learning and Gaussian barebone mechanism; MOQBHHO[38] based on *K*-Nearest Neighbor method and multiobjective HHO. However, according to no free lunch theory,[39] no single algorithm can perform best in all optimization problems. Most of the above-mentioned heuristic algorithms are able to obtain good robustness but difficult to get small root-mean-square error (RMSE) in PV cell extraction problems. At the same time, the data utilized by the heuristic algorithms may produce data bias during collection or processing, making the population highly susceptible to erroneous decision-making processes in a given context, thus affecting the accuracy of PV cell model parameter identification. Therefore, to achieve accurate identification of PV model parameters, PV model modeling in different environments needs to be considered, and at the same time, the algorithm parameters need to be reasonably set or efficient search strategies need to be introduced to improve its search accuracy and robustness, which makes the PV parameter identification problem challenging.

The SCA,[31] one of the most popular algorithms, has been proposed and widely used in optimization problems in different engineering fields. However, the SCA method occasionally presents the defects of poor exploration ability and insufficient development degree in the solution process, and it relies too much on the global destination agent of the population, so the method cannot obtain reliable and stable model parameters in the process of parameter identification of the PV cell model. Chen et al.[40] proposed a new enhanced sine–cosine algorithm (ESCA), which combines opposition-based learning (OBL) scheme and NMs concept on top of SCA. Although OBL and NMs can improve population diversification and agent

exploration capabilities, the method of selecting elite agent as offspring evolution after population merging will cause the method to lose high-precision solutions, which will inevitably lead to premature convergence, and it is difficult to ensure accurate identification of PV cell models. To enhance the performance of SCA in PV parameter identification problems. A multi strategy combinatorial hybrid algorithm named ESCA is proposed. In ESCA, the algorithm adopts a modified position update mechanism to make full use of the information of average position and optimal position of the populations, which significantly improves the degree of information exchange between populations and exploration ability. To maintain the diversity of the population in the search process, a personal destination agent mutation mechanism is proposed to ensure that the algorithm can generate more mutated individuals that are favorable to the direction of the population. Finally, the competitive selection mechanism is adopted to ensure that the optimal individuals can be in the population during each iteration of the algorithm, which improves the convergence ability of the algorithm. To verify the practicality and feasibility of the algorithm, the proposed method is compared with eight existing popular methods used to extract the parameters of three PV-diode models (*SDM*, *DDM*, and *TDM*) and three PVM models (Photowatt-PWP201, STM6-40/36, and STP6-120/36). The experimental results show that the proposed method is able to obtain competitive results and can effectively extract the parameters of six different PV models.

To summarize, the contributions of this article are as follows:

- A multi strategy SCA, ESAC, is proposed to extract parameters of the PV cell model.
- The average position of the population is introduced in the cosine evolution process of SCA instead of the global destination agent to provide more favorable search areas and directions for the population.
- Randomly select two agents from the population and perform mutation operations based on fitness information to ensure the balance between exploration and utilization in the population, and a competitive selection mechanism is used to effectively improve the mining ability of the algorithm near the global optimal solution.
- The parameters of SDM, DDM, TDM, and PVM model PV cell models were extracted using the proposed method and the existing popular methods.

Under the following topics, the rest of the paper is organized. Section 2 describes the PV problem formulation, Section 3 gives a brief description of SCA, Section 4 presents the ESCA, Section 5 presents the experimental results and discussions, and conclusions are given at the end.

2 | PHOTOVOLTAIC PROBLEM FORMULATION

According to the measured current–voltage (*I–V*) relationship of solar cells and PVMs, the parameter identification models are mainly divided into SDM, DDM, TDM, and PVM. The model and objective function are described as follows.

2.1 | SDM

The SDM, as shown in Figure 1, has the characteristics of simple structure and accurate. SDM consists of a current source, a shunt resistor, and a series resistor. The current source is connected in parallel with the diode, the shunt resistor is used to shunt the leakage current, and the series resistance represents the load current-related loss. According to the Current Law of Kirchhoff, the output current is expressed as follows[41]:

$$I = I_{ph} - I_{cd} - I_{sh}, \tag{1}$$

where I is the output current, I_{ph} is the photocurrent, I_{cd} is the current of the diode, and I_{sh} points to the current through the shunt resistance. Depending on the diode equation of Shockley, I_{cd} is defined by Equation (2), and I_{sh} is obtained by Equation (3), as follows:

$$I_{cd} = I_{sd} \times \left[\exp\left(\frac{q \times (V + R_S \times I)}{n \times k \times T}\right) - 1\right], \tag{2}$$

$$I_{sh} = \frac{V + R_S \times I}{R_{sh}}, \tag{3}$$

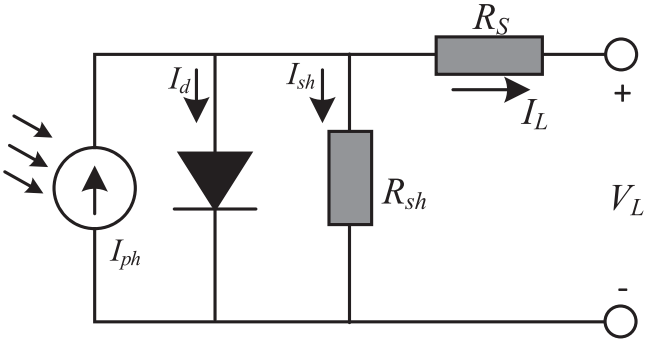

FIGURE 1 The equivalent circuit model of the single-diode model.

where I_{sd} is the reverse saturation current of diode, V is the output voltage, q points to the electron charge, k points to the Boltzmann constant, T stands for the cell temperature in Kelvin, n is the ideality factor of diode, and R_S and R_{sh} is the series and shunt resistances, respectively. Then, the output current can be rewritten as

$$I = I_{ph} - I_{sd} \times \left[\exp\left(\frac{q \times (V + R_S \times I)}{n \times k \times T}\right) - 1\right] - \frac{V + R_S \times I}{R_{sh}}. \quad (4)$$

It can be seen from the above formula that five parameters (I_{ph}, I_{sd}, R_S, R_{sh}, and n) of SDM need to be identified to obtain the calculated current value, to further reflect the performance of PV cells.

2.2 | DDM

To consider the load current loss in the depletion region, Chen et al.[42] introduced an additional diode in parallel with the current source based on SDM to show better performance, as shown in Figure 2, named the DDM. The DDM equivalent circuit diagram is shown in Figure 2, and the output current I is defined as follows[43]:

$$\begin{aligned} I &= I_{ph} - I_{cd1} - I_{cd2} - I_{sh} \\ &= I_{ph} - I_{sd1}\left[\exp\left(\frac{q \times (V + R_S \times I}{n_1 \times k \times T}\right) - 1\right] \\ &\quad - I_{sd2}\left[\exp\left(\frac{q \times (V + R_S \times I}{n_2 \times k \times T}\right) - 1\right] \\ &\quad - \frac{V + R_S \times I}{R_{sh}}, \end{aligned} \quad (5)$$

where I_{cd1} and I_{cd2} are the currents of the two diodes connected in parallel with the current source, respectively. I_{sd1} and I_{sd2} represent the diffusion and saturation currents of diodes, respectively. n_1 and n_2 are the diffusion and recombination ideality factors of diodes, respectively. It can be seen that there are seven important parameters (I_{ph}, I_{sd1}, I_{sd2}, R_S, R_{sh}, n_1, and n_2) that need to be estimated.

2.3 | TDM

The TDM adds a parallel diode based on the DDM, which has better performance than DDM and SDM. As shown in Figure 3, the output current I is defined as follows[44]:

$$\begin{aligned} I &= I_{ph} - I_{cd1} - I_{cd2} - I_{cd3} - I_{sh} \\ &= I_{ph} - I_{sd1}\left[\exp\left(\frac{q \times (V + R_S \times I}{n_1 \times k \times T}\right) - 1\right] \\ &\quad - I_{sd2}\left[\exp\left(\frac{q \times (V + R_S \times I}{n_2 \times k \times T}\right) - 1\right] \\ &\quad - I_{sd3}\left[\exp\left(\frac{q \times (V + R_S \times I}{n_3 \times k \times T}\right) - 1\right] \\ &\quad - \frac{V + R_S \times I}{R_{sh}}, \end{aligned} \quad (6)$$

where I_{sd3} and n_3 denote the current through the third diode and the diode ideality factor, respectively. And the definitions of other parameters are equivalent to DDM. Therefore, there are nine parameters (I_{ph}, I_{sd1}, I_{sd2}, I_{sd3}, R_S, R_{sh}, n_1, n_2, and n_3) that need to be evaluated that play a vital role in TDM.

2.4 | PVM

The PVM model consists of a series of parallel and/or series PV cells, in Figure 4. For a PVM composed of an SDM, the output current I is defined as follows[45]:

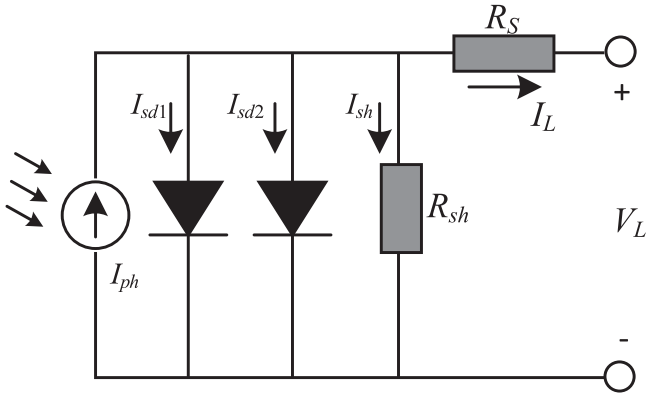

FIGURE 2 The equivalent circuit model of the double-diode model.

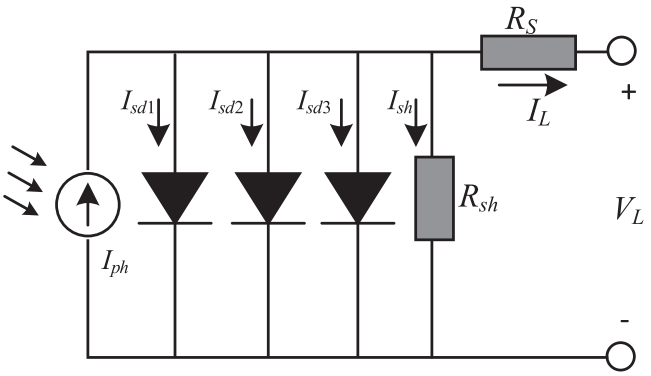

FIGURE 3 The equivalent circuit model of the three-diode model.

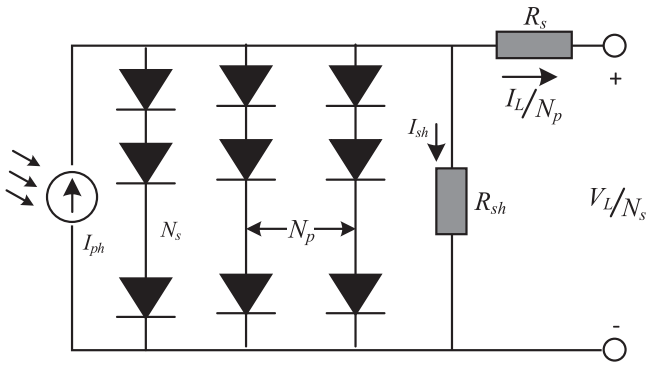

FIGURE 4 The equivalent circuit model of the photovoltaic module model.

$$I = I_{ph}N_p - I_{sd} N_p \times \left[\exp\left(\frac{q \times (V/N_s + R_S \times I/N_p)}{n \times k \times T}\right) - 1\right] - \frac{V/N_s + R_S \times I/N_p}{R_{sh} \times N_s/N_p}, \quad (7)$$

where N_p and N_s represent the number of solar cells connected in series and parallel, respectively. From Equation (7), it can be observed that PVM involves five unknown parameters (I_{ph}, I_{sd}, R_S, R_{sh}, and n) to obtain the actual behavior of the solar module.

2.5 | Problem formulation

In the solar PV model parameter identification problem, it is necessary to find the optimal parameter combination to minimize the error value between the simulated data and the measured data. Therefore, the objective functions of SDM, DDM, and TDM are calculated by Equations (8)–(10). And the objective function of PVM can be computed according to Equation (11) as follows:

$$\begin{cases} f(V, I, \boldsymbol{X}) = I_{ph} - I_{sd} \times \left[\exp\left(\frac{q \times (V + R_S \times I)}{n \times k \times T}\right) - 1\right] - \frac{V + R_S \times I}{R_{sh}} - I, \\ \boldsymbol{X} = \{I_{ph}, I_{sd}, R_S, R_{sh}, n\}, \end{cases} \text{SDM} \quad (8)$$

$$\begin{cases} f(V, I, \boldsymbol{X}) = I_{ph} - I_{sd1}\left[\exp\left(\frac{q \times (V + R_S \times I)}{n_1 \times k \times T}\right) - 1\right] - I_{sd2}\left[\exp\left(\frac{q \times (V + R_S \times I)}{n_2 \times k \times T}\right) - 1\right] - \frac{V + R_S \times I}{R_{sh}} - I, \\ \boldsymbol{X} = \{I_{ph}, I_{sd1}, R_S, R_{sh}, n_1, I_{sd2}, n_2\}, \end{cases} \text{DDM} \quad (9)$$

$$\begin{cases} f(V, I, \boldsymbol{X}) = I_{ph} - I_{sd1}\left[\exp\left(\frac{q \times (V + R_S \times I)}{n_1 \times k \times T}\right) - 1\right] - I_{sd2}\left[\exp\left(\frac{q \times (V + R_S \times I)}{n_2 \times k \times T}\right) - 1\right] - I_{sd3}\left[\exp\left(\frac{q \times (V_L + R_S \times I}{n_3 \times k \times T}\right) - 1\right] - \frac{V + R_S \times I}{R_{sh}} - I, \\ \boldsymbol{X} = \{I_{ph}, I_{sd1}, R_S, R_{sh}, n_1, I_{sd2}, n_2, I_{sd3}, n_3\}, \end{cases} \text{TDM} \quad (10)$$

$$\begin{cases} f(V, I, \boldsymbol{X}) = I_{ph}N_p - I_{sd}N_p \times \left[\exp\left(\frac{q \times (V/N_s + R_S \times I/N_p)}{n \times k \times T}\right) - 1\right] - \frac{V_L/N_s + R_S \times I_L/N_p}{R_{sh} \times N_s/N_p} - I, \\ \boldsymbol{X} = \{I_{ph}, I_{sd}, R_S, R_{sh}, n\}, \end{cases} \text{PVM} \quad (11)$$

where $\boldsymbol{X}$ symbolizes the unknown parameter vector. Then, the total difference between measured and simulated data can be quantified by defining the RMSE, *RMSE* is defined as follows:

$$RMSE(\boldsymbol{X}) = \sqrt{\frac{1}{K}\sum_{k=1}^{K} f(V, I, \boldsymbol{X})^2}, \quad (12)$$

where K represents the number of pairs of V–I in the simulated data.

3 | SINE–COSINE ALGORITHM

The SCA is a population-based global optimization heuristic algorithm proposed by Mirjalili in 2016,[31] which has the advantages of simple structure, high efficiency, and strong versatility. The detailed execution process of SCA is described in Algorithm 1. Similar to most high-performance heuristic algorithms, SCA starts the optimization process by randomly generating a series of random agents and evaluating the fitness of the agents.[46] Subsequently, SCA investigates the search space by randomly selecting sine and cosine oscillator models to allow any agent in the population to explore and exploit around a continuously updated global destination agent. Meanwhile, the four important parameters r_1, r_2, r_3, and r_4 of SCA play an important role in the movement of agent to the next position. Finally, when the counter reaches the maximum threshold or other conditions are met, the search process is stopped and the global destination agent found so far is taken as the optimal solution for the

population. As shown in Figure 5, the SCA performs the optimization process through the two-stage position update equation combining sine and cosine functions, which is expressed as follows[47]:

$$X_{ij}^{t+1} = \begin{cases} X_{ij}^{t} + r_1 \cdot \sin(r_2) \times |r_3 \cdot P_j^t - X_{ij}^t|, & r_4 < 0.5, \\ X_{ij}^{t} + r_1 \cdot \cos(r_2) \times |r_3 \cdot P_j^t - X_{ij}^t|, & \text{else}, \end{cases} \tag{13}$$

where X_{ij}^{t+1} symbolizes the positions of ith agent in jth dimension at $(t+1)$th iteration; P_j^t symbolizes the position of global destination agent in jth dimension at kth iteration; r_2 is the random number in the interval $[0, 2\pi]$; r_3 is the random number in the interval $[0, 2]$, which indicates the degree of information exchange between $X_{ij}{}^t$ and P_j^t; r_4 is the random number in the interval $[0, 1]$; $||$ denotes the absolute value; the parameter r_1 symbolizes the movement degree of next position of the agent as evolution progresses, as follows:

$$r_1 = a \cdot \left(1 - \frac{t}{T}\right), \tag{14}$$

where a symbolizes the constant number, $a = 2.0$ in the original literature; t symbolizes the number of current iterations; T symbolizes the maximum number of iterations.

Algorithm 1. The pseudocode of SCA.

1. Randomly initialize the set of agents within the search space
2. **Do**
3. Evaluate the fitness of each candidate agent via the fitness function
4. Update the global destination agent $\boldsymbol{P}^t$ found so far//$\boldsymbol{P}^t$ symbolizes the position vector of destination agent
5. Update the parameter of r_1, r_2, r_3, and r_4
6. Perform position update by Equation (13)
7. **While** $t < T$
8. **Return** the global destination agent $\boldsymbol{P}^t$ obtained so far as the final solution

4 | THE ENHANCED SINE–COSINE ALGORITHM

4.1 | Motivations

Standard SCA utilizes sine and cosine functions and the experience information of the global destination agent to update the position of agent in the population. Although this concept has a faster convergence rate than traditional methods, it does not guarantee that the algorithm can find the optimal position of the problem in each execution for problems represented by multimodal forms. Therefore, it is necessary to take measures to improve the ability of SCA to avoid local optimum. In addition, since the global destination agent of the algorithm exists in a form independent of the population after each evolutionary update, it cannot be guaranteed that the position information of the agent after each update is like beneficial to the population. Moreover, Although SCA has been successfully applied in many fields such as image recognition, path planning, and the power system, few scholars have used SCA to solve the parameter identification considerations of PV cell models. On the basis of the above analysis, this paper aims to develop an ESCA that combines a modified position

(Continues)

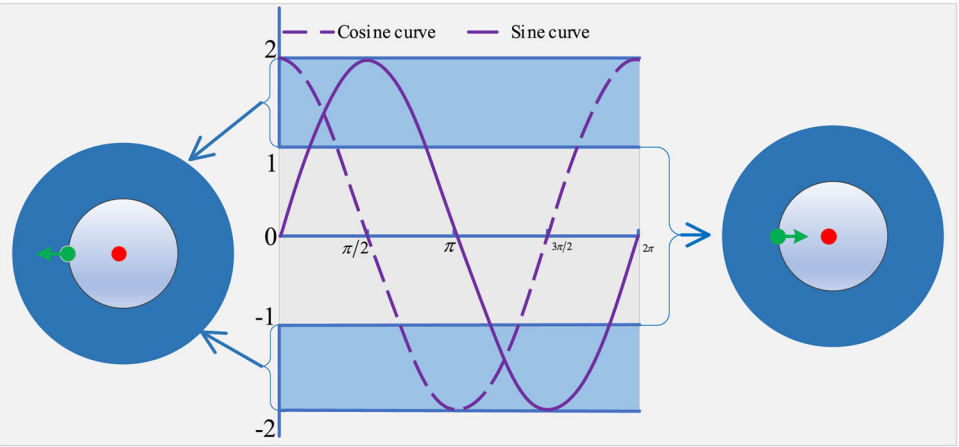

FIGURE 5 The search principle of sine–cosine algorithm.

update mechanism, personal destination agent mutation mechanism, and competitive selection mechanism to accurately identify unknown parameters under different PV cell models. The core idea of ESCA is discussed as follows.

4.2 | The modified position update mechanism

In SCA, the agents in the population search only by emphasizing and weakening the relationship between global destination agents, which causes the agents in the population to converge quickly and enter the exploration process prematurely. In addition, the algorithm does not use the average position information of the population, which has an important impact on the exploration ability of the population. Therefore, a modified position update mechanism is introduced to update the agent location of SCA. Specifically, in the two-stage location update of the original SCA, the population average location is substituted for the global destination agent in the cosine search stage, while the sine search stage still uses the local destination agent to guide agent location updates. This ensures that the algorithm can simultaneously use the information of the global destination agent and the population center to obtain a new agent location. The modified position update mechanism is defined as follows:

$$Y_{ij}^{t} = \begin{cases} X_{ij}^{t} + r_1 \cdot \sin(r_2) \times |r_3 \cdot P_j^t - X_{ij}^t|, & r_4 < 0.5, \\ X_{ij}^{t} + r_1 \cdot \cos(r_2) \times |r_3 \cdot X_{ave,j}^t - X_{ij}^t|, & \text{else} \end{cases} \tag{15}$$

$$X_{ave,j}^{t} = \frac{\sum_{i=1}^{N} X_{ij}^{t}}{N}, \tag{16}$$

where Y_{ij}^{t} symbolizes the positions of the ith intermediate agent in the jth dimension at $(k+1)$th iteration; $X_{ave,j}^{t}$ denotes the average position of the population in the jth dimension at the tth iteration, N denotes the number of the population size; to ensure that the algorithm has a balance between exploration and exploitation, r_3 is adjusted by introducing parameter r_1, which is redefined as follows:

$$r_3 = r_1 \cdot rand(0,1) = a \cdot \left(1 - \frac{t}{T}\right) \cdot rand(0,1), \tag{17}$$

where $rand(0,1)$ is the random number in the interval $[0,1]$.

4.3 | The personal destination agent mutation mechanism

In the process of population evolution, agent with higher performance are expected to find better potential areas, and the maintenance of population diversity is particularly important to ensure the accuracy of results. Considering that mutation is a powerful way to increase population diversity, a personal destination agent[48] mutation mechanism is proposed, as shown in Equation (18). Specifically, the importance of two randomly selected agents is determined by the fitness of the agents, and the agent with better fitness will be used as the basic agent, while the poorer agent and the personal destination agent generate the difference vector through standard normally distributed. Through the above operations, the population can be guaranteed to search towards the optimal solution while maintaining diversity.

$$X_{ij}^{t+1} = \begin{cases} Y_{In1,j}^{t} + N(0,1) \cdot (pbest_{ij}^{t} - Y_{In2,j}^{t}) & \text{if } F(Y_{In1}^{t}) < F(Y_{In2}^{t}), \\ Y_{In2,j}^{t} + N(0,1) \cdot (pbest_{ij}^{t} - Y_{In1,j}^{t}) & \text{else,} \end{cases} \tag{18}$$

where $In1$ and $In2$ are the index of the agent random selected from the population; $N(0,1)$ symbolizes the standard normally distributed random numbers; $pbest_{ij}^{t}$ symbolizes the positions of ith personal destination agent in jth dimension at tth iteration; $F(Y_{In1,j}^{t})$ and $F(Y_{In2}^{t})$ symbolizes the fitness value of Y_{In1}^{t} and Y_{In2}^{t}, respectively.

4.4 | Competitive selection mechanism

In the population-based heuristic algorithm, the success rate of the search mainly depends on the existence form of the global destination agent, and the global destination agent itself has more information about the potential search direction. However, the global destination agent of the standard SCA algorithm is stored in the form of an independent of the population after each update, and it cannot guarantee that there is a globally optimal agent in the population during each evolution process, which greatly affects the search capabilities of SCA. To this end, the competitive selection mechanism is adopted to ensure that the optimal destination agent remains in the population forever, and at the same time select the offspring population that is beneficial to the evolution

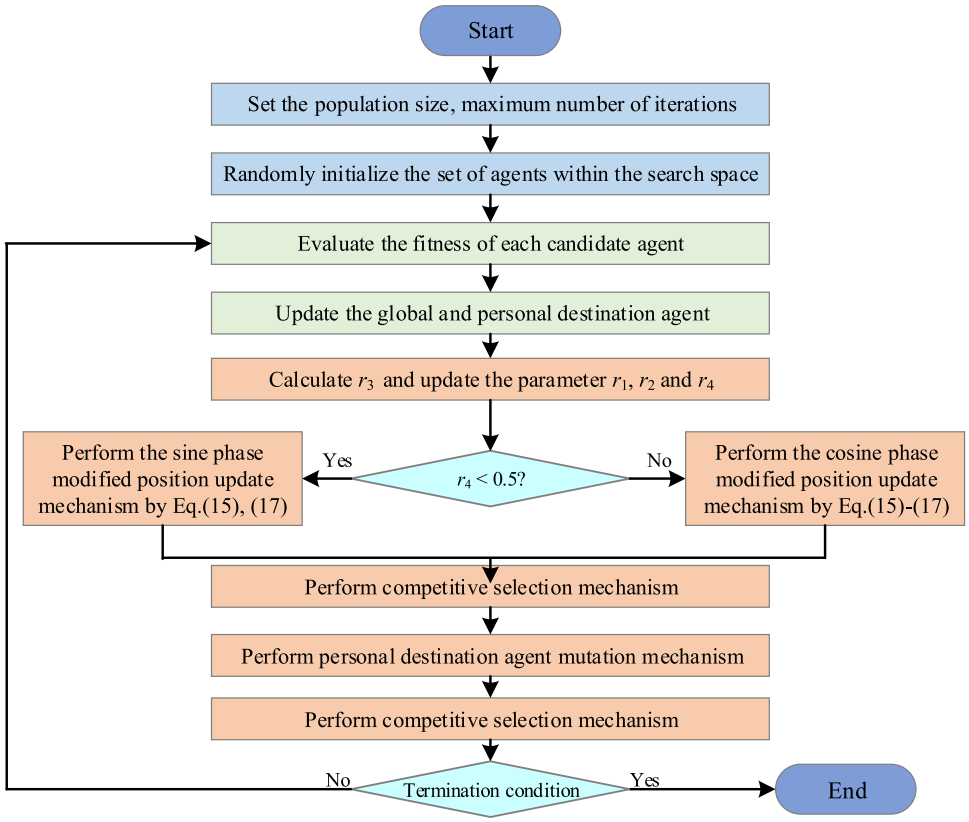

FIGURE 6 Flowchart of enhanced sine–cosine algorithm.

of the population. Only when the position information of the new agent generated is better than the parent generation, it can enter the offspring population. The competitive selection mechanism is expressed as follows:

$$X_i^{t+1} = \begin{cases} X_i^{t+1} & \text{if } F(X_i^{t+1}) < F(X_i^t), \\ X_i^t & \text{else}, \end{cases} \tag{19}$$

where $F(X_i^{t+1})$ and $F(X_i^t)$ symbolize the fitness of X_i^{t+1} and X_i^t, respectively.

4.5 | Framework of the proposed algorithm

The proposed method in this paper improves the performance level of SCA by introducing the modified position update mechanism, the personal destination agent mutation mechanism, and the competitive selection mechanism. The proposed ESCA avoids the diversity reduction, local optimum stagnation, and unfair distribution between exploration and exploitation exhibited by standard SCA during population evolution.

TABLE 1 Hyperparameter settings for different methods.

Algorithm	Parameters
CS	$N = 50$; $Discovery\_rate = 0.25$
EO	$N = 50$; $Gp = 0.5$; $V = 1.0$
GOTLBO	$N = 50$; $Jr = 1.0$
IJAYA	$N = 50$
SCA	$N = 50$; $a = 2.0$
HHO	$N = 50$
HGS	$N = 50$; $LH = 100$
RIME	$N = 50$; $W = 10$
ESCA	$N = 50$; $a = 2.0$

Abbreviations: CS, cuckoo search; EO, equilibrium optimizer; ESCA, enhanced sine–cosine algorithm; GOTLBO, generalized oppositional teaching learning-based optimization; HGS, hunger games search; HHO, Harris Hawks Optimization; IJAYA, improved JAYA; RIME, rime optimization algorithm; SCA, sine–cosine algorithm.

On the basis of the above, Algorithm 2 gives the pseudocode of ESCA, and the flowchart of ESCA is further displayed in Figure 6. It can be observed that ESCA improves the original structure of SCA. Although the global destination agent in the cosine function search

stage is replaced by the average position of the population, the algorithm does not add additional parameters that need to be set.

The complexity of ESCA mainly comes from the modified position update mechanism, the personal destination agent mutation mechanism, and the competitive selection mechanism. First, the complexity level of the modified position update mechanism is $O(N \times D)$. Then, the complexity level of the personal destination agent mutation mechanism is $O(N \times D)$, the complexity level of the competitive selection mechanism is $O(N)$. Therefore, the total complexity level of ESCA is $O(N \times (2 \times D + 1))$. In the same way, the original SCA can be obtained The complexity mainly comes from location update and fitness evaluation, and the total complexity level of SCA is $O(N \times (D + 1))$. From the above, it can be seen that the proposed method does not significantly increase the algorithm complexity compared with the original SCA.

Algorithm 2. The pseudocode of enhanced sine–cosine algorithm.

1. Randomly initialize the set of agents within the search space
2. Evaluate the fitness of each candidate agent via the fitness function
3. Update the agent of $\boldsymbol{P}^t$ and $\boldsymbol{pbest}_i^t$ found so far//$\boldsymbol{P}^t$ and $\boldsymbol{pbest}_i^t$ symbolizes the position vector of global and personal destination agent
4. **Do**
5. Calculate r_3 by Equation (17) and update the parameters r_1, r_2, and r_4
6. Perform modified position update mechanism by Equation (15)
7. Perform competitive selection mechanism by Equation (19)
8. Perform personal destination agent mutation mechanism by Equation (18)
9. Perform competitive selection mechanism by Equation (19)

TABLE 2 Lower bound (LB) and upper bound (UB) of different parameters for various models.

	SDM/ DDM/TDM		Photowatt-PWP201		STM6-40/36		STP6-120/36	
Parameter	**LB**	**UB**	**LB**	**UB**	**LB**	**UB**	**LB**	**UB**
I_{ph} (A)	0	1	0	2	0	2	0	8
R_S (Ω)	0	0.5	0	2	0	0.36	0	0.36
R_{sh} (Ω)	0	100	0	2000	0	1000	0	1500
I_{sd}, I_{sd1}, I_{sd2}, I_{sd3} (μA)	0	1	0	50	0	50	0	50
n, n_1, n_2, n_3	1	2	1	50	1	60	1	50

Abbreviations: DDM, double-diode model; SDM, single-diode model; TDM, three-diode model.

TABLE 3 Optimal parameter identification results on SDM.

Algorithm	$\boldsymbol{I_{ph}}$ **(A)**	$\boldsymbol{I_{sd}}$ **(μA)**	$\boldsymbol{R_S}$ **(Ω)**	$\boldsymbol{R_{sh}}$ **(Ω)**	$\boldsymbol{n}$	***RMSE***
CS	0.76074778	0.24678461	0.03758856	50.50012482	1.45446758	1.14418026E−03
EO	0.76077553	0.32302243	0.03637707	53.71865690	1.48118410	9.86021878E−04
GOTLBO	0.76065928	0.33704647	0.03615550	55.09211722	1.48548444	9.94635974E−04
IJAYA	0.76076936	0.32234758	0.03638670	53.68197447	1.48097893	9.86200477E−04
SCA	0.75925538	0.84089171	0.03433525	29.92100334	1.58740240	1.03259007E−02
HHO	0.76398980	0.79403864	0.03168023	37.86569398	1.57858045	3.24482213E−03
HGS	0.70133627	0.37244782	0.00000000	70.66573835	1.50521406	6.11538897E−02
RIME	0.76110624	0.36234857	0.03580975	51.74440078	1.49294624	1.04842748E−03
ESCA	0.76077553	0.32302082	0.03637709	53.71852554	1.48118359	**9.86021878E−04**

Note: The bold value is the optimal indicator result in the selected algorithm.

Abbreviations: CS, cuckoo search; EO, equilibrium optimizer; ESCA, enhanced sine–cosine algorithm; GOTLBO, generalized oppositional teaching learning-based optimization; HGS, hunger games search; HHO, Harris Hawks Optimization; IJAYA, improved JAYA; RIME, rime optimization algorithm; RMSE, root-mean-square error; SCA, sine–cosine algorithm; SDM, single-diode model.

10. Update the destination agent $\boldsymbol{P}^t$ and $\boldsymbol{pbest}_i^t$ found so far//$\boldsymbol{P}^t$ and $\boldsymbol{pbest}_i^t$ symbolizes the position vector of global and personal destination agent
11. **While** $t < T$
12. **Return** the global destination agent $\boldsymbol{P}^t$ obtained so far as the terminal solution

5 | EXPERIMENTAL RESULTS AND DISCUSSIONS

To verify the performance of the proposed method on SDM, DDM, TDM, and PVM models. First, the current and voltage data sets of 26 pairs of commercial RTC France PV cell measured under the irradiance of 1000 W/m^2 and the temperature of 33°C are selected as the measurement data of SDM, DDM, and TDM to evaluate the unknown parameters of the model.[49] Further, under the irradiance of 1000 W/m^2, the current and voltage data collected by Photowatt-PWP 201, single-crystal STM6-40/36, and polycrystalline STP6-120/36 module cells at 45°C, 51°C, and 55°C were adopted as measurement data to evaluated with unknown parameters of PVM model.[50] To be more convincing, the eight most popular methods so far, such as cuckoo search algorithm (CS),[51] equilibrium optimizer (EO),[52] generalized oppositional teaching learning-based optimization (GOTLBO),[42] improved JAYA (IJAYA),[53] HHO,[29] HGS,[25] RIME,[30] and SCA, are introduced as control methods for comparison. To

TABLE 4 Comparative results between measured and simulated data on the single-diode model.

	Measured data		Simulated current data			Simulated power data	
Item	*V* (V)	*I* (A)	*I* (A)	*IAE* (A)	*IRE*	*P* (W)	*PAE* (W)
1	−0.2057	0.7640	7.64087704E−01	8.77037665E−05	1.14795506E−02	−1.57172841E−01	−1.80406648E−05
2	−0.1291	0.7620	7.62663086E−01	6.63086128E−04	8.70191769E−02	−9.84598044E−02	−8.56044191E−05
3	−0.0588	0.7605	7.61355307E−01	8.55307114E−04	1.12466419E−01	−4.47676921E−02	−5.02920583E−05
4	0.0057	0.7605	7.60153991E−01	−3.46009027E−04	−4.54975709E−02	4.33287775E−03	−1.97225145E−06
5	0.0646	0.7600	7.59055209E−01	−9.44791152E−04	−1.24314625E−01	4.90349665E−02	−6.10335084E−05
6	0.1185	0.7590	7.58042345E−01	−9.57654798E−04	−1.26173228E−01	8.98280179E−02	−1.13482094E−04
7	0.1678	0.7570	7.57091654E−01	9.16539452E−05	1.21075225E−02	1.27039980E−01	1.53795320E−05
8	0.2132	0.7570	7.56141365E−01	−8.58635199E−04	−1.13426050E−01	1.61209339E−01	−1.83061025E−04
9	0.2545	0.7555	7.55086873E−01	−4.13127243E−04	−5.46826265E−02	1.92169609E−01	−1.05140883E−04
10	0.2924	0.7540	7.53663878E−01	−3.36121707E−04	−4.45784757E−02	2.20371318E−01	−9.82819870E−05
11	0.3269	0.7505	7.51390967E−01	8.90966615E−04	1.18716404E−01	2.45629707E−01	2.91256986E−04
12	0.3585	0.7465	7.47353852E−01	8.53851536E−04	1.14380648E−01	2.67926356E−01	3.06105776E−04
13	0.3873	0.7385	7.40117222E−01	1.61722210E−03	2.18987420E−01	2.86647400E−01	6.26350118E−04
14	0.4137	0.7280	7.27382225E−01	−6.17774848E−04	−8.48591825E−02	3.00918027E−01	−2.55573455E−04
15	0.4373	0.7065	7.06972651E−01	4.72651483E−04	6.69004222E−02	3.09159140E−01	2.06690493E−04
16	0.4590	0.6755	6.75280152E−01	−2.19848475E−04	−3.25460363E−02	3.09953590E−01	−1.00910450E−04
17	0.4784	0.6320	6.30758272E−01	−1.24172759E−03	−1.96475884E−01	3.01754758E−01	−5.94042479E−04
18	0.4960	0.5730	5.71928358E−01	−1.07164170E−03	−1.87022984E−01	2.83676466E−01	−5.31534281E−04
19	0.5119	0.4990	4.99607019E−01	6.07018665E−04	1.21647027E−01	2.55748833E−01	3.10732855E−04
20	0.5265	0.4130	4.13648792E−01	6.48792205E−04	1.57092544E−01	2.17786089E−01	3.41589096E−04
21	0.5398	0.3165	3.17510110E−01	1.01010962E−03	3.19149960E−01	1.71391957E−01	5.45257174E−04
22	0.5521	0.2120	2.12154939E−01	1.54939196E−04	7.30845265E−02	1.17130742E−01	8.55419302E−05
23	0.5633	0.1035	1.02251312E−01	−1.24868811E−03	−1.20646194E+00	5.75981640E−02	−7.03386011E−04
24	0.5736	−0.0100	−8.71754154E−03	1.28245846E−03	−1.28245846E+01	−5.00038183E−03	7.35618172E−04
25	0.5833	−0.1230	−1.25507413E−01	−2.50741256E−03	2.03854680E+00	−7.32084737E−02	−1.46257375E−03
26	0.5900	−0.2100	−2.08472326E−01	1.52767375E−03	−7.27463692E−01	−1.22998672E−01	9.01327514E−04

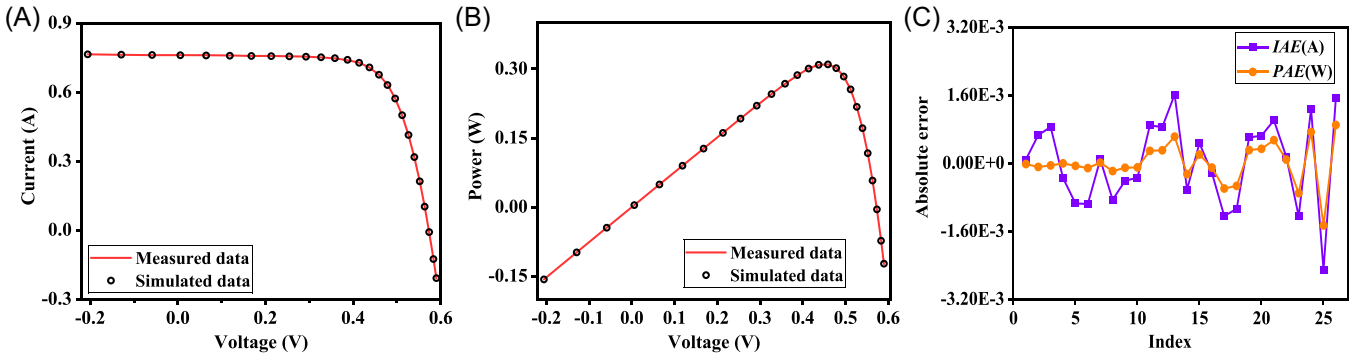

FIGURE 7 Simulated and measured characteristics of the single-diode model ((a). I-V curve of ESCA in SDM; (b). P-V curve of ESCA in SDM; (c). IAE and PAE of ESCA in SDM).

TABLE 5 Optimal parameter identification results on DDM.

Algorithm	I_{ph} (A)	I_{sd1} (μA)	R_S (Ω)	R_{sh} (Ω)	n_1	I_{sd2} (μA)	n_2	*RMSE*
CS	0.76202901	0.32196584	0.03624947	50.73874616	1.48390511	0.29254580	1.91942165	1.62711298E−03
EO	0.76078432	1.00000000	0.03691497	56.15211273	1.98435380	0.19052159	1.43701125	9.83420973E−04
GOTLBO	0.76108829	0.28433526	0.03654930	54.04166758	1.47049446	0.09841192	1.80915443	1.04074930E−03
IJAYA	0.76053035	0.32239154	0.03640696	55.79493100	1.48095675	0.00000000	1.51620108	9.95109982E−04
SCA	0.75858713	0.29396341	0.03888605	100.00000000	1.47009615	0.00687071	2.00000000	5.76916967E−03
HHO	0.75895938	0.14036298	0.03703851	97.43287474	1.44523082	0.30935244	1.58160836	2.28752934E−03
HGS	0.78586254	0.89872782	0.04167216	24.17798973	1.85317782	0.69838680	1.58729776	3.00800272E−02
RIME	0.76104377	0.00613340	0.03610796	52.47993905	1.98481344	0.34073192	1.48667149	1.00627382E−03
ESCA	0.76078108	0.22597446	0.03674043	55.48543978	1.45101684	0.74934591	2.00000000	**9.82484852E−04**

Note: The bold value is the optimal indicator result in the selected algorithm.

Abbreviations: CS, cuckoo search; DDM, double-diode model; EO, equilibrium optimizer; ESCA, enhanced sine–cosine algorithm; GOTLBO, generalized oppositional teaching learning-based optimization; HGS, hunger games search; HHO, Harris Hawks Optimization; IJAYA, improved JAYA; RIME, rime optimization algorithm; RMSE, root-mean-square error; SCA, sine–cosine algorithm.

ensure a fair comparison between algorithms, the hyper-parameters of each algorithm are consistent with the original literature settings. The maximum number of function evaluations for all methods was set to 30,000 and 30 independent running experiments were performed. Table 1 shows the parameter settings of different methods, and the problem boundary settings of different models are given in Table 2.

5.1 | Results on SDM, DDM, and TDM

5.1.1 | Results on SDM

This section elaborates on the unknown parameter extraction performance of ESCA in the SDM problem. *IAE* and *IRE* were introduced to represent the absolute error and relative error between the simulated current and the measured current, and *PAE* to represent the absolute error between the simulated power and the measured power, as follows:

$$\begin{cases} IAE = I_{simulated} - I_{measured}, \\ IRE = \frac{(I_{simulated} - I_{measured})\,\%}{I_{simulated}}, \\ PAE = P_{simulated} - P_{measured}, \end{cases} \tag{20}$$

Table 3 lists the comparison results of the six heuristic algorithms on the optimal RMSE for the SDM problem. It can be seen that the results of the original SCA perform worse than other methods because it gives larger RMSE results; however, the proposed method can give satisfactory RMSE results, and its results are better than CS, EO, GOTLBO, IJAYA, SCA, HHO, HGS, and RIME obtained results.

To further demonstrate the error of the proposed method at different voltages, Table 4 shows the current–voltage (*I*–*V*) characteristic results obtained by

TABLE 6 Comparative results between measured and simulated data on the double-diode model.

	Measured data		Simulated current data			Simulated power data	
Item	*V* (V)	*I* (A)	*I* (A)	*IAE* (A)	*IRE* (A)	*P* (W)	*PAE* (W)
1	−0.2057	0.7640	7.63983412E−01	−1.65877551E−05	−2.17117213E−03	−1.57151388E−01	3.41210122E−06
2	−0.1291	0.7620	7.62604096E−01	6.04095862E−04	7.92776722E−02	−9.84521888E−02	−7.79887758E−05
3	−0.0588	0.7605	7.61337698E−01	8.37697993E−04	1.10150952E−01	−4.47666566E−02	−4.92566420E−05
4	0.0057	0.7605	7.60173787E−01	−3.26212521E−04	−4.28944801E−02	4.33299059E−03	−1.85941137E−06
5	0.0646	0.7600	7.59107680E−01	−8.92320306E−04	−1.17410567E−01	4.90383561E−02	−5.76438917E−05
6	0.1185	0.7590	7.58121419E−01	−8.78580773E−04	−1.15755043E−01	8.98373882E−02	−1.04111822E−04
7	0.1678	0.7570	7.57188613E−01	1.88612943E−04	2.49158445E−02	1.27056249E−01	3.16492518E−05
8	0.2132	0.7570	7.56243606E−01	−7.56393876E−04	−9.99199307E−02	1.61231137E−01	−1.61263174E−04
9	0.2545	0.7555	7.55177301E−01	−3.22699202E−04	−4.27133292E−02	1.92192623E−01	−8.21269469E−05
10	0.2924	0.7540	7.53722353E−01	−2.77647006E−04	−3.68232104E−02	2.20388416E−01	−8.11839846E−05
11	0.3269	0.7505	7.51399134E−01	8.99133980E−04	1.19804661E−01	2.45632377E−01	2.93926898E−04
12	0.3585	0.7465	7.47301443E−01	8.01443363E−04	1.07360129E−01	2.67907567E−01	2.87317446E−04
13	0.3873	0.7385	7.40010661E−01	1.51066116E−03	2.04558045E−01	2.86606129E−01	5.85079068E−04
14	0.4137	0.7280	7.27246953E−01	−7.53046727E−04	−1.03440485E−01	3.00862065E−01	−3.11535431E−04
15	0.4373	0.7065	7.06850299E−01	3.50298642E−04	4.95822565E−02	3.09105636E−01	1.53185596E−04
16	0.4590	0.6755	6.75210543E−01	−2.89456690E−04	−4.28507314E−02	3.09921639E−01	−1.32860621E−04
17	0.4784	0.6320	6.30760758E−01	−1.23924189E−03	−1.96082577E−01	3.01755947E−01	−5.92853319E−04
18	0.4960	0.5730	5.71994733E−01	−1.00526703E−03	−1.75439273E−01	2.83709388E−01	−4.98612448E−04
19	0.5119	0.4990	4.99706135E−01	7.06135021E−04	1.41510024E−01	2.55799571E−01	3.61470517E−04
20	0.5265	0.4130	4.13733672E−01	7.33672321E−04	1.77644630E−01	2.17830778E−01	3.86278477E−04
21	0.5398	0.3165	3.17546205E−01	1.04620523E−03	3.30554576E−01	1.71411442E−01	5.64741584E−04
22	0.5521	0.2120	2.12122996E−01	1.22995611E−04	5.80167975E−02	1.17113106E−01	6.79058767E−05
23	0.5633	0.1035	1.02163276E−01	−1.33672365E−03	−1.29152044E+00	5.75485736E−02	−7.52976432E−04
24	0.5736	−0.0100	−8.79175105E−03	1.20824895E−03	−1.20824895E+01	−5.04294840E−03	6.93051598E−04
25	0.5833	−0.1230	−1.25543435E−01	−2.54343497E−03	2.06783331E+00	−7.32294856E−02	−1.48358562E−03
26	0.5900	−0.2100	−2.08371589E−01	1.62841076E−03	−7.75433694E−01	−1.22939238E−01	9.60762347E−04

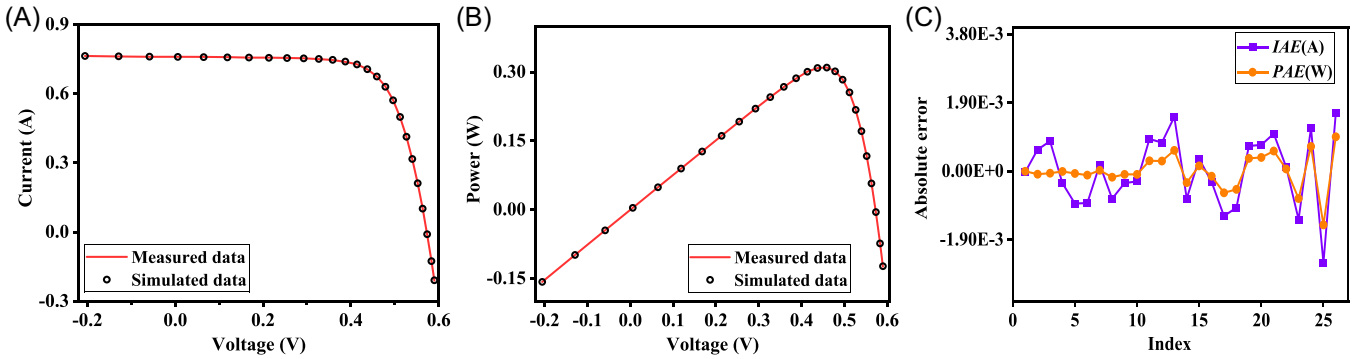

FIGURE 8 Simulated and measured characteristics of the double-diode model ((a). I-V curve of ESCA in DDM; (b). P-V curve of ESCA in DDM; (c). IAE and PAE of ESCA in DDM).

bringing the unknown parameter results obtained by ESCA into the SDM model. It can be seen that the current and voltage values of the simulation results obtained through experiments are very close to the measured values because their error values are small, which shows that the proposed method is reliable. Figure 7 further shows the *I–V* and power–voltage (*P–V*) characteristic curves of the SDM and the error curves of the voltage points obtained by using ESCA. It can be seen that the current and power simulation values obtained by calculation are highly consistent with the measured values in all voltage points. The above fully demonstrates that the proposed ESCA method can accurately describe the actual behavior of solar cells through the SDM model.

5.1.2 | Results on double-diode mode

In this section, DDM is selected to verify the performance of the proposed method. Table 5 shows the comparison between ESCA and eight competing methods on the optimal results. In the comparison of the best results of all methods, the proposed method obtained the smallest RMSE value of 9.82484852E−04, which was reduced by 6.44628128E−04, 9.36121000E−07, 5.82644480E−05, 1.26251300E−05, and 4.78668482E−03 compared with CS, EO, GOTLBO, IJAYA, and SCA, respectively.

Considering the detailed error situation of each voltage position, Table 6 shows the statistical results of current and voltage errors obtained for the proposed method. Among them, the maximum forward error and reverse maximum error of current are 1.62841076E−03 and 2.54343497E−03, respectively; the forward maximum error and reverse maximum error of power are 9.60762347E−04 and 1.48358562E−03, respectively. These error values are the smallest among all methods, indicating that ESCA can accurately extract unknown parameters on the DDM model. Similarly, Figure 8 shows *I–V*, *P–V*, and the corresponding errors of measured and simulated values more intuitively. It can be seen from the figure that the observed current and voltage are highly consistent with the simulated values, which fully demonstrates that the proposed method has a better performance in the DDM problem.

5.1.3 | Results on TDM

This section discusses in detail the performance of ESCA on the experimental results for the TDM problem. Table 7 shows the optimal parameter identification

TABLE 7 Optimal parameter identification results on TDM.

Algorithm	I_{ph} (A)	I_{sd1} (μA)	R_S (Ω)	R_{sh} (Ω)	n_1	I_{sd2} (μA)	n_2	I_{sd3} (μA)	n_3	*RMSE*
CS	0.76100088	0.27647703	0.03640745	64.96997790	1.46911272	0.36521529	1.99962775	0.08409404	1.86533478	1.21678238E−03
EO	0.76077553	0.00000000	0.03637710	53.71843678	1.99999920	0.32301991	1.48118331	0.00000000	1.00000022	9.86021878E−04
GOTLBO	0.76145873	0.32544207	0.03589784	55.59781490	1.48456916	0.00000000	1.32809381	0.09255861	1.76645553	1.16586781E−03
IJAYA	0.76088448	0.03521599	0.03638102	52.65370719	1.39234230	0.02140826	1.91100542	0.31552870	1.51272856	1.00516637E−03
SCA	0.74927673	0.00000000	0.02967581	64.91667064	2.00000000	0.00000000	2.00000000	0.67672929	1.55960466	1.23112779E−02
HHO	0.76124991	0.34028632	0.03505230	68.88155945	1.49932640	0.22029414	1.75014618	0.01922151	1.50038445	1.35984016E−03
HGS	0.78586031	0.09957050	0.01034141	75.11641551	2.00000000	0.02629296	1.90542404	1.00000000	1.60315324	4.78785593E−02
RIME	0.76111077	0.14978504	0.03809427	47.08972960	1.41296059	0.55953123	2.00000000	0.28742100	2.00000000	1.16111161E−03
ESCA	0.76078108	0.74934806	0.03674043	55.48544245	2.00000000	0.22597419	1.45101674	0.00000000	1.91869707	**9.82484852E−04**

Note: The bold value is the optimal indicator result in the selected algorithm.

Abbreviations: CS, cuckoo search; EO, equilibrium optimizer; ESCA, enhanced sine–cosine algorithm; GOTLBO, generalized oppositional teaching learning-based optimization; HGS, hunger games search; HHO, Harris Hawks Optimization; IJAYA, improved JAYA; RIME, rime optimization algorithm; RMSE, root-mean-square error; SCA, sine–cosine algorithm; TDM, three-diode model.

TABLE 8 Comparative results between measured and simulated data on the three-diode model.

	Measured data		Simulated current data			Simulated power data	
Item	*V* (V)	*I* (A)	*I* (A)	*IAE* (A)	*IRE* (A)	*P* (W)	*PAE* (W)
1	−0.2057	0.7640	7.63983412E−01	−1.65876076E−05	−2.17115283E−03	−1.57151388E−01	3.41207089E−06
2	−0.1291	0.7620	7.62604096E−01	6.04096076E−04	7.92777003E−02	−9.84521888E−02	−7.79888034E−05
3	−0.0588	0.7605	7.61337698E−01	8.37698267E−04	1.10150988E−01	−4.47666567E−02	−4.92566581E−05
4	0.0057	0.7605	7.60173788E−01	−3.26212194E−04	−4.28944371E−02	4.33299059E−03	−1.85940951E−06
5	0.0646	0.7600	7.59107680E−01	−8.92319934E−04	−1.17410518E−01	4.90383561E−02	−5.76438677E−05
6	0.1185	0.7590	7.58121420E−01	−8.78580369E−04	−1.15754989E−01	8.98373882E−02	−1.04111774E−04
7	0.1678	0.7570	7.57188613E−01	1.88613356E−04	2.49158990E−02	1.27056249E−01	3.16493211E−05
8	0.2132	0.7570	7.56243607E−01	−7.56393485E−04	−9.99198791E−02	1.61231137E−01	−1.61263091E−04
9	0.2545	0.7555	7.55177301E−01	−3.22698878E−04	−4.27132863E−02	1.92192623E−01	−8.21268644E−05
10	0.2924	0.7540	7.53722353E−01	−2.77646799E−04	−3.68231829E−02	2.20388416E−01	−8.11839240E−05
11	0.3269	0.7505	7.51399134E−01	8.99134029E−04	1.19804667E−01	2.45632377E−01	2.93926914E−04
12	0.3585	0.7465	7.47301443E−01	8.01443244E−04	1.07360113E−01	2.67907567E−01	2.87317403E−04
13	0.3873	0.7385	7.40010661E−01	1.51066092E−03	2.04558012E−01	2.86606129E−01	5.85078973E−04
14	0.4137	0.7280	7.27246953E−01	−7.53046999E−04	−1.03440522E−01	3.00862064E−01	−3.11535543E−04
15	0.4373	0.7065	7.06850298E−01	3.50298477E−04	4.95822332E−02	3.09105636E−01	1.53185524E−04
16	0.4590	0.6755	6.75210543E−01	−2.89456643E−04	−4.28507244E−02	3.09921639E−01	−1.32860599E−04
17	0.4784	0.6320	6.30760758E−01	−1.23924162E−03	−1.96082534E−01	3.01755947E−01	−5.92853189E−04
18	0.4960	0.5730	5.71994733E−01	−1.00526663E−03	−1.75439202E−01	2.83709388E−01	−4.98612246E−04
19	0.5119	0.4990	4.99706135E−01	7.06135411E−04	1.41510102E−01	2.55799571E−01	3.61470717E−04
20	0.5265	0.4130	4.13733673E−01	7.33672507E−04	1.77644675E−01	2.17830779E−01	3.86278575E−04
21	0.5398	0.3165	3.17546205E−01	1.04620511E−03	3.30554538E−01	1.71411442E−01	5.64741520E−04
22	0.5521	0.2120	2.12122995E−01	1.22995173E−04	5.80165911E−02	1.17113106E−01	6.79056351E−05
23	0.5633	0.1035	1.02163276E−01	−1.33672428E−03	−1.29152104E+00	5.75485732E−02	−7.52976785E−04
24	0.5736	−0.0100	−8.79175149E−03	1.20824851E−03	−1.20824851E+01	−5.04294866E−03	6.93051343E−04
25	0.5833	−0.1230	−1.25543435E−01	−2.54343504E−03	2.06783337E+00	−7.32294857E−02	−1.48358566E−03
26	0.5900	−0.2100	−2.08371589E−01	1.62841145E−03	−7.75434024E−01	−1.22939237E−01	9.60762756E−04

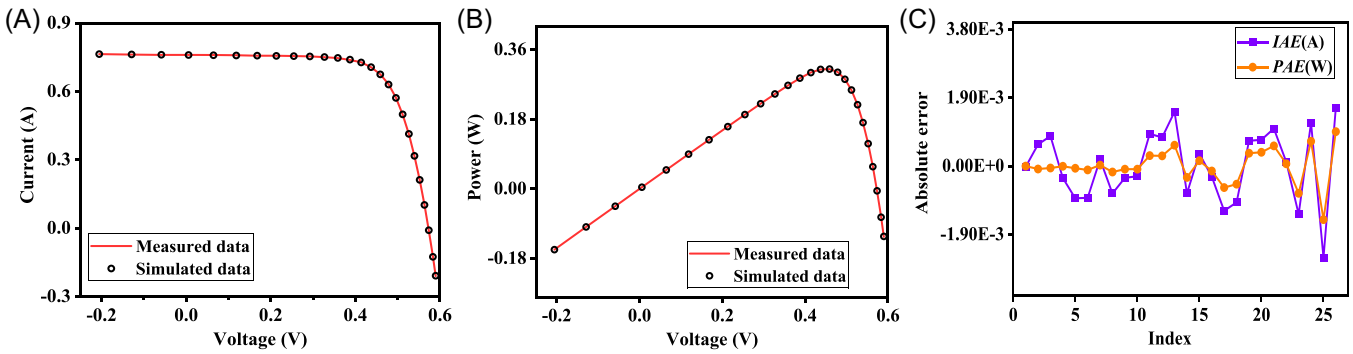

FIGURE 9 Simulated and measured characteristics of the three-diode model ((a). I-V curve of ESCA in TDM; (b). P-V curve of ESCA in TDM; (c). IAE and PAE of ESCA in TDM).

TABLE 9 Optimal parameter identification results on Photowatt-PWP201.

Algorithm	I_{ph} (A)	I_{sd} (μA)	R_S (Ω)	R_{sh} (Ω)	n	*RMSE*
CS	1.03060112	3.43950382	1.20341570	964.02398313	48.59544764	2.42919122E−03
EO	1.03051409	3.48236600	1.20126792	982.01765643	48.64294804	2.42507487E−03
GOTLBO	1.03036215	3.55083545	1.19914318	1006.55636522	48.71732298	2.42596066E−03
IJAYA	1.03046876	3.49208784	1.20111630	985.52660379	48.65363299	2.42528840E−03
SCA	1.04250361	4.82682809	1.10143263	347.50364159	50.00000000	8.47406240E−03
HHO	1.03224896	3.84726388	1.23761450	1046.37027067	49.01797177	5.63727726E−03
HGS	1.15735823	5.37568640	1.01664719	749.24434933	50.00000000	1.04138682E−01
RIME	1.02909720	3.60055439	1.20038544	1193.32831968	48.76586331	2.45590476E−03
ESCA	1.03051430	3.48226293	1.20127101	981.98230604	48.64283488	**2.42507487E−03**

Note: The bold value is the optimal indicator result in the selected algorithm.

Abbreviations: CS, cuckoo search; EO, equilibrium optimizer; ESCA, enhanced sine–cosine algorithm; GOTLBO, generalized oppositional teaching learning-based optimization; HGS, hunger games search; HHO, Harris Hawks Optimization; IJAYA, improved JAYA; RIME, rime optimization algorithm; RMSE, root-mean-square error; SCA, sine–cosine algorithm.

TABLE 10 Comparative results between measured and simulated data on Photowatt-PWP201.

	Measured data		Simulated current data		Simulated power data	
Item	V (V)	I (A)	I (A)	*IAE* (A)	P (W)	*PAE* (W)
1	0.1248	1.0315	1.02911916E+00	−2.38083896E−03	1.28434071E−01	−2.97128703E−04
2	1.8093	1.03	1.02738107E+00	−2.61892705E−03	1.85884058E+00	−4.73842471E−03
3	3.3511	1.026	1.02574180E+00	−2.58203212E−04	3.43736334E+00	−8.65264783E−04
4	4.7622	1.022	1.02410715E+00	2.10715472E−03	4.87700309E+00	1.00346922E−02
5	6.0538	1.018	1.02229180E+00	4.29180455E−03	6.18875013E+00	2.59817264E−02
6	7.2364	1.0155	1.01993068E+00	4.43068090E−03	7.38062638E+00	3.20621793E−02
7	8.3189	1.014	1.01636311E+00	2.36310573E−03	8.45502304E+00	1.96584402E−02
8	9.3097	1.01	1.01049615E+00	4.96151373E−04	9.40741602E+00	4.61902044E−03
9	10.2163	1.0035	1.00062897E+00	−2.87103025E−03	1.02227257E+01	−2.93313063E−02
10	11.0449	0.988	9.84548378E−01	−3.45162154E−03	1.08742384E+01	−3.81228147E−02
11	11.8018	0.963	9.59521676E−01	−3.47832402E−03	1.13240829E+01	−4.10504844E−02
12	12.4929	0.9255	9.22838818E−01	−2.66118218E−03	1.15289331E+01	−3.32458829E−02
13	13.1231	0.8725	8.72599662E−01	9.96624802E−05	1.14512126E+01	1.30788069E−03
14	13.6983	0.8075	8.07274263E−01	−2.25736745E−04	1.10582850E+01	−3.09220965E−03
15	14.2221	0.7265	7.28336478E−01	1.83647753E−03	1.03584742E+01	2.61185671E−02
16	14.6995	0.6345	6.37138000E−01	2.63799954E−03	9.36561002E+00	3.87772743E−02
17	15.1346	0.5345	5.36213063E−01	1.71306270E−03	8.11537022E+00	2.59265188E−02
18	15.5311	0.4275	4.29511325E−01	2.01132452E−03	6.67078333E+00	3.12380823E−02
19	15.8929	0.3185	3.18774482E−01	2.74482479E−04	5.06625097E+00	4.36232259E−03
20	16.2229	0.2085	2.07389506E−01	−1.11049352E−03	3.36445922E+00	−1.80154253E−02
21	16.5241	0.101	9.61671717E−02	−4.83282828E−03	1.58907596E+00	−7.98581378E−02
22	16.7987	−0.008	−8.32538604E−03	−3.25386041E−04	−1.39855662E−01	−5.46606249E−03
23	17.0499	−0.111	−1.10936482E−01	6.35175273E−05	−1.89145593E+00	1.08296749E−03
24	17.2793	−0.209	−2.09247265E−01	−2.47265482E−04	−3.61564627E+00	−4.27257443E−03
25	17.4885	−0.303	−3.00863586E−01	2.13641369E−03	−5.26165283E+00	3.73626707E−02

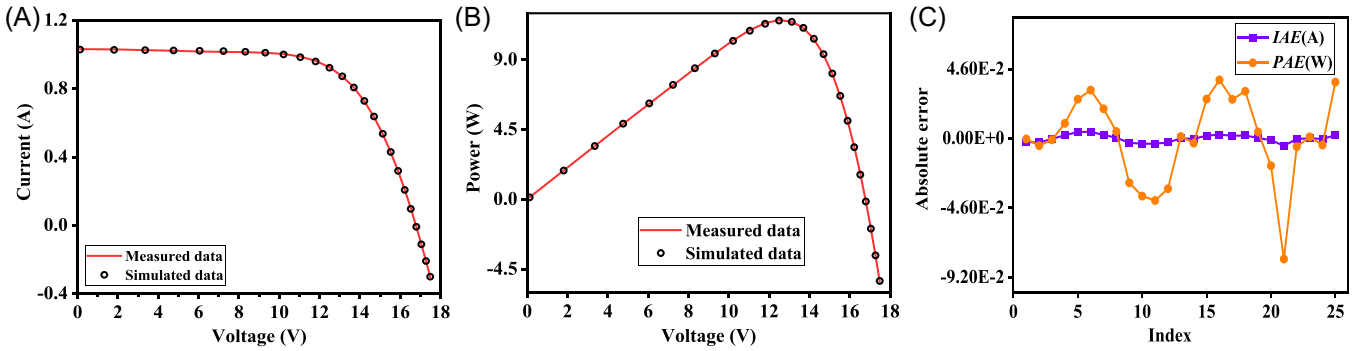

FIGURE 10 Parameter identification of *I–V* and *P–V* characteristics of Photowatt-PWP201 ((a). I-V curve of ESCA in Photowatt-PWP201; (b). P-V curve of ESCA in Photowatt-PWP201; (c). IAE and PAE of ESCA in Photowatt-PWP201).

TABLE 11 Optimal parameter identification results on STM6-40/36.

Algorithm	I_{ph} (A)	I_{sd} (μA)	R_S (Ω)	R_{sh} (Ω)	n	*RMSE*
CS	1.65260527	7.96019277	0.00000000	803.20758578	1.70749208	5.53077082E−03
EO	1.66155158	5.50510527	0.00000000	23.55866367	1.65852899	3.32985094E−03
GOTLBO	1.66130183	5.05487029	0.00058180	23.19688887	1.64752386	3.16482257E−03
IJAYA	1.66196725	3.25408167	0.00207315	20.62845142	1.59229454	2.38169154E−03
SCA	1.65470969	7.23602513	0.00000000	209.14730049	1.69157525	8.86690022E−03
HHO	1.65564762	6.18236977	0.00000000	55.05366640	1.67338494	4.29068457E−03
HGS	1.49383556	50.00000000	0.00000000	898.82054736	2.74002047	3.40350683E−01
RIME	1.65794653	10.68906756	0.00000000	1000.00000000	1.74971226	7.70400955E−03
ESCA	1.66390478	1.73865694	0.00427377	15.92829431	1.52030292	**1.72981371E−03**

Note: The bold value is the optimal indicator result in the selected algorithm.

Abbreviations: CS, cuckoo search; EO, equilibrium optimizer; ESCA, enhanced sine–cosine algorithm; GOTLBO, generalized oppositional teaching learning-based optimization; HGS, hunger games search; HHO, Harris Hawks Optimization; IJAYA, improved JAYA; RIME, rime optimization algorithm; RMSE, root-mean-square error; SCA, sine–cosine algorithm.

results of ESCA and comparison methods CS, EO, GOTLBO, IJAYA, SCA HHO, HGS, and RIME. From the results, it can be clearly seen that ESCA has the smallest RMSE among all methods, which indicates that the proposed method has the best potential for the TDM problem.

On the basis of the competitive results of ESCA in Table 7, Table 8 further shows the error results of the measured and simulated values obtained by the proposed method under TDM with respect to current and power. It can be clearly seen that the error results obtained by ESCA under TDM are similar to the results of SDM and DDM, and the error values are very small. The absolute value of the maximum error of the current is 2.54343504E−03, and the absolute value of the maximum error of the voltage is 1.48358566E−03. The above shows that the proposed method has better performance for TDM problems. From the TDM simulation and experimental characteristic curves shown in Figure 9, it can also be seen that the simulation characteristic curve data obtained by ESCA matches the experimental data very well, which is consistent with the performance of ESCA on DDM, which also shows that the proposed method can correctly evaluate the unknown parameters of TDM.

5.2 | Experiments on different PVMs

5.2.1 | Results on Photowatt-PWP201

Likewise, ESCA was first used on the Photowatt-PWP201 PVM to verify its performance on the PVM. ESCA is compared in detail with eight other competing methods on the obtained optimal parameter results. Table 9 shows the RMSE values of the optimal results and the optimal parameter information. It can be seen

TABLE 12 Comparative results between measured and simulated data on STM6-40/36.

	Measured data		Simulated current data		Simulated power data	
Item	*V* (V)	*I* (A)	*I* (A)	*IAE* (A)	*P* (W)	*PAE* (W)
1	0	1.663	1.66345826E+00	4.58255464E−04	0.00000000E+00	0.00000000E+00
2	0.118	1.663	1.66325231E+00	2.52307184E−04	1.96263772E−01	2.97722477E−05
3	2.237	1.661	1.65955081E+00	−1.44919392E−03	3.71241515E+00	−3.24184681E−03
4	5.434	1.653	1.65391470E+00	9.14696736E−04	8.98737246E+00	4.97046207E−03
5	7.26	1.65	1.65056591E+00	5.65911579E−04	1.19831085E+01	4.10851806E−03
6	9.68	1.645	1.64543060E+00	4.30602582E−04	1.59277682E+01	4.16823299E−03
7	11.59	1.64	1.63923353E+00	−7.66465339E−04	1.89987167E+01	−8.88333328E−03
8	12.6	1.636	1.63371269E+00	−2.28730637E−03	2.05847799E+01	−2.88200602E−02
9	13.37	1.629	1.62728581E+00	−1.71419430E−03	2.17568112E+01	−2.29187779E−02
10	14.09	1.619	1.61831357E+00	−6.86426756E−04	2.28020382E+01	−9.67175299E−03
11	14.88	1.597	1.60309004E+00	6.09004231E−03	2.38539798E+01	9.06198296E−02
12	15.59	1.581	1.58158837E+00	5.88373645E−04	2.46569627E+01	9.17274513E−03
13	16.4	1.542	1.54233059E+00	3.30588026E−04	2.52942216E+01	5.42164363E−03
14	16.71	1.524	1.52119263E+00	−2.80736919E−03	2.54191289E+01	−4.69111392E−02
15	16.98	1.5	1.49919474E+00	−8.05258730E−04	2.54563267E+01	−1.36732932E−02
16	17.13	1.485	1.48527527E+00	2.75267039E−04	2.54427653E+01	4.71532438E−03
17	17.32	1.465	1.46565424E+00	6.54239321E−04	2.53851314E+01	1.13314250E−02
18	17.91	1.388	1.38758937E+00	−4.10634117E−04	2.48517255E+01	−7.35445704E−03
19	19.08	1.118	1.11839137E+00	3.91374116E−04	2.13389074E+01	7.46741814E−03
20	21.02	0	−2.48108056E−05	−2.48108056E−05	−5.21523133E−04	−5.21523133E−04

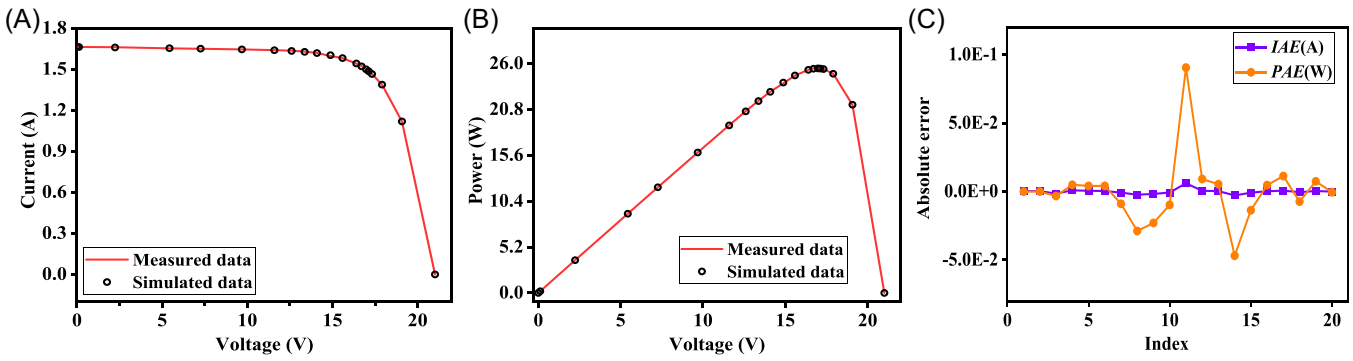

FIGURE 11 Parameter identification of *I–V* and *P–V* characteristics of STM6-40/36 ((a). I-V curve of ESCA in STM6-40/36; (b). P-V curve of ESCA in STM6-40/36; (c). IAE and PAE of ESCA in STM6-40/36).

that in terms of the optimal parameter results, except for the poor performance of SCA, other methods obtain similar results, but ESCA obtains the smallest RMSE simulation result, indicating that ESCA has the best performance.

Table 10 shows the comparison results of real data and simulated data obtained by the proposed method. It can be seen that the simulation results are similar to the measurement results, and the error values of current and power are very small. Figure 10 further shows the measurement and simulation results at each voltage value, the current and power change with the voltage, and the simulation results are all on the curve. This strongly demonstrates that ESCA performs better

TABLE 13 Optimal parameter identification results on STP6-120/36.

Algorithm	I_{ph} (A)	I_{sd} (μA)	R_S (Ω)	R_{sh} (Ω)	n	*RSME*
CS	7.48537182	13.85393490	0.00372633	1047.52219333	1.43049878	4.28686262E−02
EO	7.84781883	50.00000000	0.00000000	0.62635722	1.58410809	2.27256208E−01
GOTLBO	7.49156324	6.94659743	0.00409715	679.66933188	1.35890456	2.57708686E−02
IJAYA	7.46251814	2.92339083	0.00448696	1281.59269876	1.27912036	1.69533007E−02
SCA	7.45032950	12.76024266	0.00257904	84.93149604	1.41337968	1.40169460E−01
HHO	7.53713583	46.95707301	0.00273648	1414.80567775	1.57377089	5.42146403E−02
HGS	6.13015960	15.32613938	0.00000000	449.77823322	9.95617519	1.71535087E+00
RIME	7.44731077	1.49517883	0.00483492	1499.98984247	1.22381386	1.92959362E−02
ESCA	7.47252992	2.33499511	0.00459463	22.21990420	1.26010348	**1.66006031E−02**

Note: The bold value is the optimal indicator result in the selected algorithm.

Abbreviations: CS, cuckoo search; EO, equilibrium optimizer; ESCA, enhanced sine–cosine algorithm; GOTLBO, generalized oppositional teaching learning-based optimization; HGS, hunger games search; HHO, Harris Hawks Optimization; IJAYA, improved JAYA; RIME, rime optimization algorithm; RMSE, root-mean-square error; SCA, sine–cosine algorithm.

TABLE 14 Comparative results between measured and simulated data on STP6-120/36.

	Measured data		Simulated current data		Simulated power data	
Item	V (V)	I (A)	I (A)	*IAE* (A)	P (W)	*PAE* (W)
1	19.21	0	2.28259923E−03	2.28259923E−03	4.38487311E−02	4.38487311E−02
2	17.65	3.83	3.83334720E+00	3.34719582E−03	6.76585780E+01	5.90780063E−02
3	17.41	4.29	4.26733758E+00	−2.26624171E−02	7.42943473E+01	−3.94552682E−01
4	17.25	4.56	4.54114855E+00	−1.88514534E−02	7.83348124E+01	−3.25187570E−01
5	17.1	4.79	4.78440021E+00	−5.59978753E−03	8.18132436E+01	−9.57563667E−02
6	16.9	5.07	5.08557807E+00	1.55780688E−02	8.59462694E+01	2.63269363E−01
7	16.76	5.27	5.27482246E+00	4.82246091E−03	8.84060244E+01	8.08244448E−02
8	16.34	5.75	5.78259748E+00	3.25974778E−02	9.44876428E+01	5.32642786E−01
9	16.08	6	6.04431798E+00	4.43179786E−02	9.71926331E+01	7.12633096E−01
10	15.71	6.36	6.34712090E+00	−1.28790950E−02	9.97132694E+01	−2.02330583E−01
11	15.39	6.58	6.56654991E+00	−1.34500918E−02	1.01059203E+02	−2.06996913E−01
12	14.93	6.83	6.81361105E+00	−1.63889527E−02	1.01727213E+02	−2.44687063E−01
13	14.58	6.97	6.95770972E+00	−1.22902842E−02	1.01443408E+02	−1.79192344E−01
14	14.17	7.1	7.08757579E+00	−1.24242054E−02	1.00430949E+02	−1.76050991E−01
15	13.59	7.23	7.21738487E+00	−1.26151348E−02	9.80842603E+01	−1.71439682E−01
16	13.16	7.29	7.28399958E+00	−6.00042396E−03	9.58574344E+01	−7.89655793E−02
17	12.74	7.34	7.33134549E+00	−8.65451135E−03	9.34013415E+01	−1.10258475E−01
18	12.36	7.37	7.36318321E+00	−6.81678828E−03	9.10089445E+01	−8.42555031E−02
19	11.81	7.38	7.39599986E+00	1.59998559E−02	8.73467583E+01	1.88958298E−01
20	11.17	7.41	7.42031576E+00	1.03157614E−02	8.28849271E+01	1.15227055E−01
21	10.32	7.44	7.43908982E+00	−9.10177527E−04	7.67714070E+01	−9.39303208E−03
22	9.74	7.42	7.44676211E+00	2.67621060E−02	7.25314629E+01	2.60662912E−01
23	9.06	7.45	7.45254041E+00	2.54041032E−03	6.75200161E+01	2.30161175E−02
24	0	7.48	7.47097941E+00	−9.02058609E−03	0.00000000E+00	0.00000000E+00

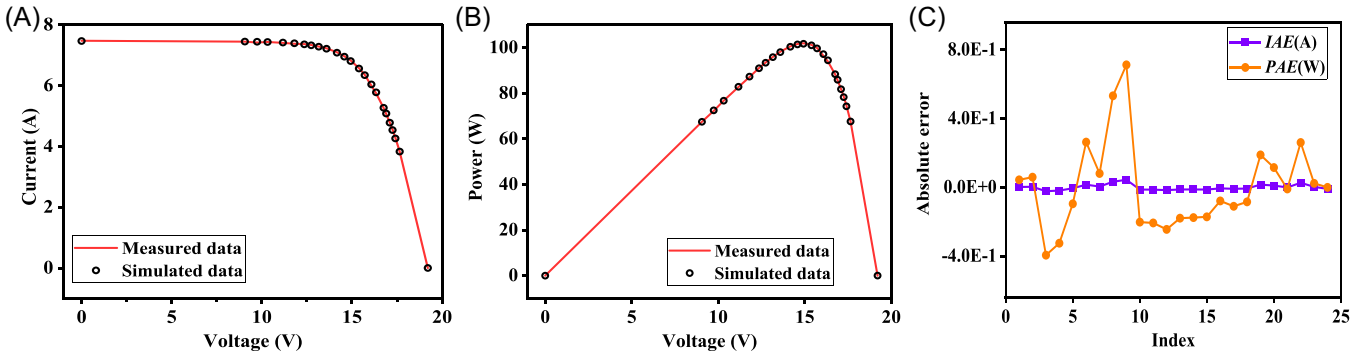

FIGURE 12 Parameter identification of *I–V* and *P–V* characteristics of STP6-120/36 ((a). I-V curve of ESCA in STP6-120/36; (b). P-V curve of ESCA in STP6-120/36; (c). IAE and PAE of ESCA in DDM).

than other methods on the Photowatt-PWP201 module.

5.2.2 | Result on STM6-40/36

For the STM6-40/36 case, Table 11 describes the optimal extraction parameter results of ESCA and other methods. It can be seen that the ESCA reduces the RMSE by 3.80095711E−03, 3.32985094E−03, 3.16482257E−03, 2.38169154E−03, and 8.86690022E−03, respectively, compared with CS, EO, GOTLBO, IJAYA, and SCA. Table 12 shows the error value results of power and current under the STM6-40/36 module. It can be seen that the error values of current and voltage are very small, and the maximum error is only 6.09004231E−03 and 9.06198296E−02 in current and voltage, respectively. Figure 11 clearly shows that the current and voltage data obtained by the proposed method are basically consistent with the experimental data. In conclusion, the proposed method can obtain the best parameter extraction results among all participating methods, proving its superiority.

5.2.3 | Result on STP6-120/36

The optimal parameter results for STP6-120/36 components are shown in Table 13. It can be seen from the table that ESCA can give a better RMSE value than other popular methods, which shows better optimal results through the reasonable exploration and exploration process of the algorithm.

Table 14 further shows the detailed error statistical results of current and power with respect to voltage under this PVM. The *IAE* value of current is between −2.26624171E−02 and 4.43179786E−02, the *PAE* value of voltage is between −3.94552682E−01 and 7.12633096E−01, which indicates that ESCA is an effective parameter evaluation method. As shown in Figure 12, the *I–V* and *P–V* curves obtained by the proposed method are in good agreement with the actual values, which also shows the advantage evaluation of the proposed method.

5.3 | Statistical results analysis

Table 15 lists the statistical results of different models of all participating algorithms after running 30 times independently. The statistical indicators of RMSE include the best value, median, mean, worst value, and SD (standard deviation), and the smaller the same indicator in the same model, the better the performance of the method. It should be noted that the SD index represents the stable performance of the algorithm repeated experiments on the model many times.

It can be seen from Table 15 that the proposed ESCA algorithm is more reliable than other popular methods in the comparison of optimal value, median, mean, and worst value. In the comparison of the standard deviation, it is only slightly lower than the EO method on the STP6-120/36 model, but it is more stable than other methods. Specifically, compared with CS, EO, GOTLBO, IJAYA, and SCA, ESCA improves the worst values in SDM by 5.72134100E−04, 5.28231000E−05, 8.69087100E−04, 3.75633100E−04, and 5.14022781 E−02; Compared with the average value of TDM, ESCA has increased by 1.74548540E−03, 6.64224000E−05, 1.13457440E−03, 2.08984400E−04, and 3.72203894E−02; and compared with the optimal value of STP6-120/36 module, ESCA has been improved by 2.62680300E−02, 2.10655600E−01, 9.17027000E−03, 3.52700000E−04, and 1.23568900E−01. Although the standard deviation of ESCA in the

TABLE 15 Statistical results obtained by various methods on different models.

Model	Indicator	CS	EO	GOTLBO	IJAYA	SCA	HHO	HGS	RIME	ESCA
SDM	Best	1.144180E−03	9.860219E−04	9.946360E−04	9.862005E−04	1.032590E−02	3.244822E−03	6.115389E−02	1.048427E−03	**9.860219E−04**
	Median	1.466873E−03	9.860219E−04	1.393479E−03	1.035920E−03	4.375105E−02	1.252429E−02	1.685635E−01	1.813824E−03	**9.860219E−04**
	Mean	1.410292E−03	9.887149E−04	1.354960E−03	1.071375E−03	3.981266E−02	1.726225E−02	1.626325E−01	1.835237E−03	**9.860219E−04**
	Worst	1.558156E−03	1.038845E−03	1.855109E−03	1.361655E−03	5.238830E−02	5.014425E−02	2.828761E−01	4.789807E−03	**9.860219E−04**
	SD	1.203038E−04	1.015200E−05	2.508336E−04	1.011046E−04	1.108050E−02	1.303683E−02	5.354635E−02	7.550408E−04	**2.384123E−17**
DDM	Best	1.627113E−03	9.834210E−04	1.040749E−03	9.951100E−04	5.769170E−03	2.287529E−03	3.008003E−02	1.006274E−03	**9.824849E−04**
	Median	2.062857E−03	**9.836794E−04**	1.493024E−03	1.084417E−03	4.252532E−02	2.357612E−02	1.591578E−01	1.870852E−03	9.843281E−04
	Mean	2.019735E−03	9.903050E−04	1.598819E−03	1.193999E−03	3.828024E−02	2.447917E−02	1.575698E−01	2.170432E−03	**9.842716E−04**
	Worst	2.596284E−03	1.128802E−03	3.145814E−03	1.611077E−03	7.118391E−02	6.492669E−02	3.029560E−01	4.032481E−03	**9.860219E−04**
	SD	2.710791E−04	2.749054E−05	4.511648E−04	1.885644E−04	1.466094E−02	1.626559E−02	6.398532E−02	8.629437E−04	**1.439012E−06**
TDM	Best	1.216782E−03	9.860219E−04	1.165868E−03	1.005166E−03	1.231128E−02	1.359840E−03	4.787856E−02	1.161112E−03	**9.824849E−04**
	Median	2.673390E−03	9.860220E−04	2.033839E−03	1.167215E−03	4.235601E−02	2.398530E−02	1.401364E−01	2.647044E−03	**9.841700E−04**
	Mean	2.734206E−03	1.055143E−03	2.123295E−03	1.197705E−03	3.820911E−02	2.598246E−02	1.513971E−01	2.596941E−03	**9.887206E−04**
	Worst	3.415761E−03	2.340130E−03	3.048678E−03	1.555244E−03	5.579173E−02	7.633688E−02	3.125249E−01	4.077853E−03	**1.111806E−03**
	SD	4.663657E−04	2.644581E−04	4.941887E−04	1.587884E−04	1.140650E−02	1.780026E−02	6.436811E−02	7.727056E−04	**2.331489E−05**
PV-PWP201	Best	2.429191E−03	2.425075E−03	2.425961E−03	2.425288E−03	8.474062E−03	5.637277E−03	1.041387E−01	2.455905E−03	**2.425075E−03**
	Median	2.580556E−03	2.425079E−03	2.545628E−03	2.448914E−03	7.477920E−02	2.134399E−02	4.129179E−01	2.623636E−03	**2.425075E−03**
	Mean	2.563372E−03	2.430085E−03	2.540190E−03	2.476086E−03	8.750816E−02	5.591559E−02	1.055858E+00	2.896274E−03	**2.425075E−03**
	Worst	2.653631E−03	2.502777E−03	2.733006E−03	2.810187E−03	2.743321E−01	2.827047E−01	7.123864E+00	5.498807E−03	**2.425075E−03**
	SD	5.828957E−05	1.625149E−05	5.726701E−05	8.194295E−05	8.096721E−02	8.120125E−02	1.575465E+00	7.519035E−04	**1.742315E−17**
STM6-40/36	Best	5.530771E−03	3.329851E−03	3.164823E−03	2.381692E−03	8.866900E−03	4.290685E−03	3.403507E−01	7.704010E−03	**1.729814E−03**
	Median	8.905259E−03	3.329851E−03	5.357230E−03	3.274131E−03	3.559508E−02	3.426386E−02	3.629742E−01	3.157331E−02	**1.729814E−03**
	Mean	9.687905E−03	3.331505E−03	5.621316E−03	3.259564E−03	1.493243E−01	1.242188E−01	3.612744E−01	3.009852E−02	**1.729814E−03**
	Worst	2.243708E−02	3.379035E−03	9.832958E−03	5.078007E−03	3.108209E−01	3.629460E−01	3.649846E−01	3.316962E−02	**1.729814E−03**
	SD	3.645577E−03	8.977330E−06	1.663841E−03	5.584482E−04	1.438256E−01	1.494115E−01	4.731292E−03	4.846695E−03	**7.206085E−18**
STP6-120/36	Best	4.286863E−02	2.272562E−01	2.577087E−02	1.695330E−02	1.401695E−01	5.421464E−02	1.715351E+00	1.929594E−02	**1.660060E−02**
	Median	5.337452E−02	2.272562E−01	4.108718E−02	2.477540E−02	3.104408E−01	1.715399E+00	1.715958E+00	5.398602E−02	**1.660060E−02**

(Continues)

TABLE 15 (Continued)

Model	Indicator	CS	EO	GOTLBO	IJAYA	SCA	HHO	HGS	RIME	ESCA
	Mean	5.311690E−02	2.272562E−01	5.656892E−02	2.548266E−02	7.668131E−01	1.426505E+00	1.717052E+00	5.038821E−02	**1.660060E−02**
	Worst	6.682037E−02	2.272562E−01	2.272793E−01	4.418140E−02	1.413123E+00	1.715470E+00	1.724119E+00	5.549470E−02	**1.660060E−02**
	SD	5.002973E−03	**9.277346E−17**	4.567991E−02	6.619357E−03	5.775988E−01	5.761511E−01	2.406595E−03	8.462449E−03	1.594007E−16

Note: The bold value is the optimal indicator result in the selected algorithm.

Abbreviations: CS, cuckoo search; DDM, double-diode model; EO, equilibrium optimizer; ESCA, enhanced sine–cosine algorithm; GOTLBO, generalized oppositional teaching learning-based optimization; HGS, hunger games search; HHO, Harris Hawks Optimization; IJAYA, improved JAYA; RIME, rime optimization algorithm; SCA, sine–cosine algorithm; SDM, single-diode model; TDM, three-diode model.

STP6-120/36 module is worse than that of EO, from the perspective of the overall distribution, the comprehensive score obtained by ESCA is much better than that of EO. Therefore, in terms of the statistical results of the PV model, ESCA has competitive convergence accuracy and more reliable parameter evaluation results.

The average central processing unit execution time of different algorithms on multiple PV models is given in Figure 13, from which it can be seen that the EO, HHO, HGS, and RIEM algorithms have relatively shorter execution times and CS, GOTLBO, IJAYA, SCA, and ESCA have relatively longer execution time. In addition, the proposed ESCA algorithm has an increase in runtime of less than 0.2 s compared to the other methods, and it can be concluded that the proposed method is able to obtain a more accurate solution in a reasonable time.

6 | DISCUSSION

In the previous sections, the proposed ESCA method is thoroughly compared with eight existing popular methods, while based on the results of parameter extraction for six different types of PV models, it can be clearly seen that the proposed method is able to obtain a more satisfactory solution than its rivals. The results show that smaller RMSE values and more stable results can be obtained by the proposed method. By comparing the results of ESCA with SCA on different models, it can be found that the proposed improved strategy can make SCA have good diversity preservation and high convergence accuracy. In conclusion, the proposed ESCA method is a promising tool for parameter extraction for complex PV models.

As the environment in which the PV cells are located in real-world environments is dynamically changing, for example, the temperature, light irradiance, and wind speed of the environment in which the PV cells are located over time is nonconstant and shading may be present. For this reason, in the future, we need to consider adequate consideration and correction of these factors in the modeling process to ensure that the model is able to take into account the impact of environmental changes on the PV system. In addition, modeling in dynamic environments leads to complexity in the internal structure of the model, which inevitably increases the difficulty of the algorithms to solve the problem. To improve the stability and accuracy of the results, a combination of traditional mathematical and heuristic algorithms for solving will be a new direction in future work.

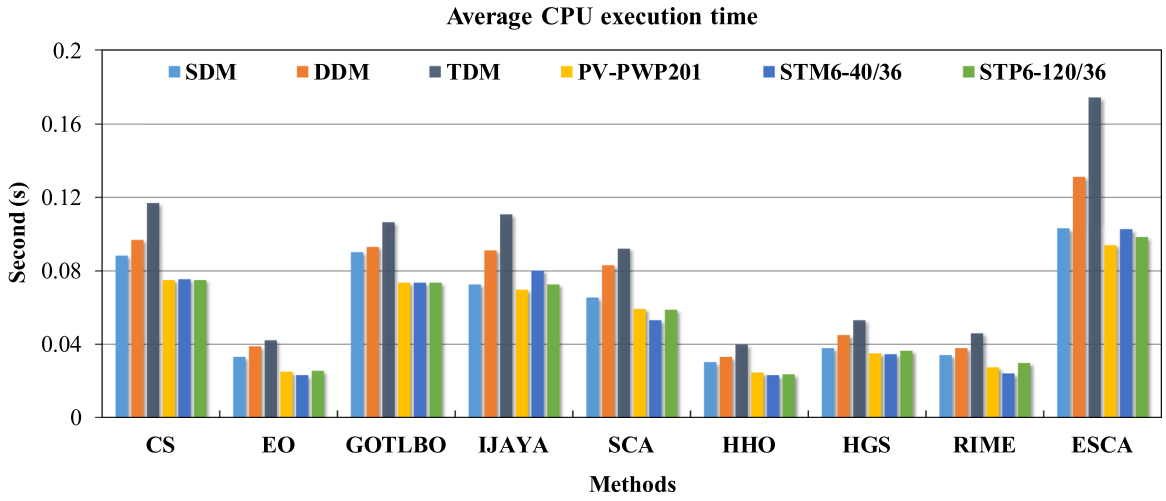

FIGURE 13 Average central processing unit execution time of different methods. CPU, central processing unit; CS, cuckoo search; DDM, double-diode model; EO, equilibrium optimizer; ESCA, enhanced sine–cosine algorithm; GOTLBO, generalized oppositional teaching learning-based optimization; HGS, hunger games search; HHO, Harris Hawks Optimization; IJAYA, improved JAYA; RIME, rime optimization algorithm; SCA, sine–cosine algorithm; SDM, single-diode model; TDM, three-diode model.

7 | CONCLUSIONS

In this paper, an enhanced ESCA is proposed to identify the critical parameters of different solar PV models with high precision. In ESCA, the average position of the population is introduced in the cosine evolution stage of the standard SCA instead of the global destination agent to provide more search directions for the agent update, effectively expand the search range, and enhance the mining ability in the exploration process. To ensure that the proposed algorithm can maintain excellent diversity during the entire search process and ensure the convergence speed of ESCA, the agent with good performance is used as the basic agent, and the agent with poor performance is differentially operated with the introduction of personal destination agents to ensure enhanced diversity of the population. Then the competitive selection mechanism is introduced to alleviate the defect that SCA does not guarantee that the updated global destination agent position remains in the population during the design process, so as to improve the population searchability.

The simulation experiments were carried out with six PV cell models: TDMs including SDM, DDM, and TDM, and three PVM models including Photowatt-PWP201, STM6-40/36, and STP6-120/36. By comparing the proposed method with existing popular methods in terms of optimal parameter results and statistical results, ESCA is verified as a candidate technique for solving PV unknown parameters. For SDM, DDM, and TDM, ESCA produces the best RMSE values of 9.860219E−04, 9.824849E−04, and 9.824849E−04, respectively, and the solution given by the proposed method is the best choice for the optimization of the parameters of the PV system when compared with the existing popular methods. Further, from the fitting characteristic curves of current–voltage (*I*–*V*) and power–voltage (*P*–*V*) of different commercial PV cells, it can be seen that the ESCA simulation results are highly consistent with the measurement data, and the results are satisfactory. The above experimental results show that the proposed method has the advantages of accuracy, effectiveness, and feasibility on the PV cell model, and it is a solution tool that cannot be ignored.

Considering the advantages of ESCA, we will utilize the proposed method to apply to the renewable energy problem with high-dimensional complex constraints. In addition, we also attempt to explore the application of ESCA in the field of short-term load forecasting and related time series forecasting problems.

ACKNOWLEDGMENTS

The writers would like to thank the editors and reviewers for their valuable comments and suggestions.

CONFLICT OF INTEREST STATEMENT

The authors declare no conflict of interest.

ORCID

Ting-ting Zhou http://orcid.org/0009-0002-9223-4922

REFERENCES

1. Yu S, Heidari AA, He C, et al. Parameter estimation of static solar photovoltaic models using Laplacian Nelder–Mead hunger games search. *Sol Energy*. 2022;242:79-104.

2. Liang J, Qiao K, Yu K, et al. Parameters estimation of solar photovoltaic models via a self-adaptive ensemble-based differential evolution. *Sol Energy*. 2020;207:336-346.
3. Gao S, Wang K, Tao S, Jin T, Dai H, Cheng J. A state-of-the-art differential evolution algorithm for parameter estimation of solar photovoltaic models. *Energy Convers Manage*. 2021; 230:113784.
4. Mahmoodzadeh A, Mohammadi M, Gharrib Noori KM, et al. Presenting the best prediction model of water inflow into drill and blast tunnels among several machine learning techniques. *Automat Constr*. 2021;127:103719.
5. Luo W, Yu X. Quasi-reflection based multi-strategy cuckoo search for parameter estimation of photovoltaic solar modules. *Sol Energy*. 2022;243:264-278.
6. Yu Y, Wang K, Zhang T, Wang Y, Peng C, Gao S. A population diversity-controlled differential evolution for parameter estimation of solar photovoltaic models. *Sustainable Energy Technol Assess*. 2022;51:101938.
7. Wang D, Sun X, Kang H, Shen Y, Chen Q. Heterogeneous differential evolution algorithm for parameter estimation of solar photovoltaic models. *Energy Rep*. 2022;8:4724-4746.
8. Yang X, Gong W. Opposition-based JAYA with population reduction for parameter estimation of photovoltaic solar cells and modules. *Appl Soft Comput*. 2021;104:107218.
9. Premkumar M, Jangir P, Ramakrishnan C, et al. An enhanced gradient-based optimizer for parameter estimation of various solar photovoltaic models. *Energy Rep*. 2022;8:15249-15285.
10. Peng L, He C, Heidari AA, et al. Information sharing search boosted whale optimizer with Nelder–Mead simplex for parameter estimation of photovoltaic models. *Energy Convers Manage*. 2022;270:116246.
11. Vickers NJ. Animal communication: when I'm calling you, will you answer too? *Curr Biol*. 2017;27:R713-R715.
12. Feng Z, Niu W, Liu S. Cooperation search algorithm: a novel metaheuristic evolutionary intelligence algorithm for numerical optimization and engineering optimization problems. *Appl Soft Comput*. 2021;98:106734.
13. Shang C, Zhou T, Liu S. Optimization of complex engineering problems using modified sine cosine algorithm. *Sci Rep*. 2022;12:20528.
14. Zhou J, Zhang Y, Zhang Y, Shang WL, Yang Z, Feng W. Parameters identification of photovoltaic models using a differential evolution algorithm based on elite and obsolete dynamic learning. *Appl Energy*. 2022;314:118877.
15. Xu B, Heidari AA, Kuang F, Zhang S, Chen H, Cai Z. Performance optimization of photovoltaic systems: reassessment of political optimization with a quantum Nelder–Mead functionality. *Sol Energy*. 2022;234:39-63.
16. Bo Q, Cheng W, Khishe M, Mohammadi M, Mohammed AH. Solar photovoltaic model parameter identification using robust niching chimp optimization. *Sol Energy*. 2022;239: 179-197.
17. Yang C, Su C, Hu H, Habibi M, Safarpour H, Amine Khadimallah M. Performance optimization of photovoltaic and solar cells via a hybrid and efficient chimp algorithm. *Sol Energy*. 2023;253:343-359.
18. El-Dabah MA, El-Sehiemy RA, Hasanien HM, Saad B. Photovoltaic model parameters identification using Northern Goshawk Optimization algorithm. *Energy*. 2023;262:125522.
19. Kharchouf Y, Herbazi R, Chahboun A. Parameter's extraction of solar photovoltaic models using an improved differential evolution algorithm. *Energy Convers Manage*. 2022;251: 114972.
20. Long W, Jiao J, Liang X, Xu M, Tang M, Cai S. Parameters estimation of photovoltaic models using a novel hybrid seagull optimization algorithm. *Energy*. 2022;249:123760.
21. Ali F, Sarwar A, Ilahi Bakhsh F, Ahmad S, Ali Shah A, Ahmed H. Parameter extraction of photovoltaic models using atomic orbital search algorithm on a decent basis for novel accurate RMSE calculation. *Energy Convers Manage*. 2023; 277:116613.
22. Xu S, Qiu H. A modified stochastic fractal search algorithm for parameter estimation of solar cells and PV modules. *Energy Rep*. 2022;8:1853-1866.
23. Wang GG, Deb S, Cui Z. Monarch butterfly optimization. *Neural Comput Appl*. 2019;31:1995-2014.
24. Wang GG. Moth search algorithm: a bio-inspired metaheuristic algorithm for global optimization problems. *Memetic Comput*. 2018;10:151-164.
25. Yang Y, Chen H, Heidari AA, Gandomi AH. Hunger games search: visions, conception, implementation, deep analysis, perspectives, and towards performance shifts. *Expert Syst Appl*. 2021;177:114864.
26. Ahmadianfar I, Heidari AA, Gandomi AH, Chu X, Chen H. RUN beyond the metaphor: an efficient optimization algorithm based on Runge Kutta method. *Expert Syst Appl*. 2021;181:115079.
27. Tu J, Chen H, Wang M, Gandomi AH. The colony predation algorithm. *J Bionic Eng*. 2021;18:674-710.
28. Ahmadianfar I, Heidari AA, Noshadian S, Chen H, Gandomi AH. INFO: an efficient optimization algorithm based on weighted mean of vectors. *Expert Syst Appl*. 2022; 195:116516.
29. Heidari AA, Mirjalili S, Faris H, Aljarah I, Mafarja M, Chen H. Harris hawks optimization: algorithm and applications. *Fut Gener Comput Syst*. 2019;97:849-872.
30. Su H, Zhao D, Heidari AA, et al. RIME: a physics-based optimization. *Neurocomputing*. 2023;532:183-214.
31. Mirjalili S. SCA: a sine cosine algorithm for solving optimization problems. *Knowl-Based Syst*. 2016;96:120-133.
32. Thawkar S, Sharma S, Khanna M, Singh L. Breast cancer prediction using a hybrid method based on butterfly optimization algorithm and ant lion optimizer. *Comput Biol Med*. 2021;139:104968.
33. Arora S, Singh S. Butterfly optimization algorithm: a novel approach for global optimization. *Soft Comput*. 2019;23: 715-734.
34. Mirjalili S. The ant lion optimizer. *Adv Eng Software*. 2015;83: 80-98.
35. Sayed GI, Soliman MM, Hassanien AE. A novel melanoma prediction model for imbalanced data using optimized SqueezeNet by bald eagle search optimization. *Comput Biol Med*. 2021;136:104712.
36. Alsattar HA, Zaidan AA, Zaidan BB. Novel meta-heuristic bald eagle search optimisation algorithm. *Artif Intell Rev*. 2020;53:2237-2264.
37. Xing J, Zhao H, Chen H, Deng R, Xiao L. Boosting whale optimizer with quasi-oppositional learning and Gaussian

barebone for feature selection and COVID-19 image segmentation. *J Bionic Eng*. 2023;20:797-818.
38. Piri J, Mohapatra P. An analytical study of modified multi-objective Harris Hawk Optimizer towards medical data feature selection. *Comput Biol Med*. 2021;135:104558.
39. Wolpert DH, Macready WG. No free lunch theorems for optimization. *IEEE Trans Evol Comput*. 1997;1:67-82.
40. Chen H, Jiao S, Heidari AA, Wang M, Chen X, Zhao X. An opposition-based sine cosine approach with local search for parameter estimation of photovoltaic models. *Energy Convers Manage*. 2019;195:927-942.
41. AlRashidi MR, AlHajri MF, El-Naggar KM, Al-Othman AK. A new estimation approach for determining the *I–V* characteristics of solar cells. *Sol Energy*. 2011;85:1543-1550.
42. Chen X, Yu K, Du W, Zhao W, Liu G. Parameters identification of solar cell models using generalized oppositional teaching learning based optimization. *Energy*. 2016;99:170-180.
43. Wolf M, Noel GT, Stirn RJ. Investigation of the double exponential in the current–voltage characteristics of silicon solar cells. *IEEE Trans Electron Devices*. 1977;ED-24:419-428.
44. Nishioka K, Sakitani N, Uraoka Y, Fuyuki T. Analysis of multicrystalline silicon solar cells by modified 3-diode equivalent circuit model taking leakage current through periphery into consideration. *Sol Energy Mater Sol Cells*. 2007;91:1222-1227.
45. Krishnan H, Islam MS, Ahmad MA, Rashid MIM. Parameter identification of solar cells using improved Archi-medes Optimization Algorithm. *OPTIK*. 2023;295:171465.
46. Abualigah L, Diabat A. Advances in sine cosine algorithm: a comprehensive survey. *Artif Intell Rev*. 2021;54:2567-2608.
47. Gabis AB, Meraihi Y, Mirjalili S, Ramdane-Cherif A. A comprehensive survey of sine cosine algorithm: variants and applications. *Artif Intell Rev*. 2021;54:5469-5540.
48. Marini F, Walczak B. Particle swarm optimization (PSO). A tutorial. *Chemom Intell Lab Syst*. 2015;149:153-165.
49. Easwarakhanthan t, Bottin J, Bouhouch I, Boutrit C. Nonlinear minimization algorithm for determining the solar cell parameters with microcomputers. *Int J Solar Energy*. 1986;4:1-12.
50. Li S, Gu Q, Gong W, Ning B. An enhanced adaptive differential evolution algorithm for parameter extraction of photovoltaic models. *Energy Convers Manage*. 2020;205:112443.
51. Yang XS, Deb S. Cuckoo search: recent advances and applications. *Neural Comput Appl*. 2014;24:169-174.
52. Faramarzi A, Heidarinejad M, Stephens B, Mirjalili S. Equilibrium optimizer: a novel optimization algorithm. *Knowl-Based Syst*. 2020;191:105190.
53. Yu K, Liang JJ, Qu BY, Chen X, Wang H. Parameters identification of photovoltaic models using an improved JAYA optimization algorithm. *Energy Convers Manage*. 2017;150:742-753.

How to cite this article: Zhou T-t, Shang C. Parameter identification of solar photovoltaic models by multi strategy sine–cosine algorithm. *Energy Sci Eng*. 2024;12:1422-1445. doi:10.1002/ese3.1673